NAVAL POSTGRADUATE SCHOOL

MONTEREY, CALIFORNIA

THESIS

ROBOTIC SPACECRAFT HOPPING: APPLICATION AND ANALYSIS

by

Katrina P. Alsup

December 2018

Thesis Advisor: Marcello Romano
Co-Advisor: Josep Virgili-Llop (contractor)

THIS PAGE INTENTIONALLY LEFT BLANK

REPORT DOCUMENTATION PAGE			*Form Approved OMB No. 0704-0188*

1. AGENCY USE ONLY *(Leave blank)*	**2. REPORT DATE** December 2018	**3. REPORT TYPE AND DATES COVERED** Master's thesis

4. TITLE AND SUBTITLE ROBOTIC SPACECRAFT HOPPING: APPLICATION AND ANALYSIS	**5. FUNDING NUMBERS** RMM4L
6. AUTHOR(S) Katrina P. Alsup	
7. PERFORMING ORGANIZATION NAME(S) AND ADDRESS(ES) Naval Postgraduate School Monterey, CA 93943-5000	**8. PERFORMING ORGANIZATION REPORT NUMBER**
9. SPONSORING / MONITORING AGENCY NAME(S) AND ADDRESS(ES) NRO, VA	**10. SPONSORING / MONITORING AGENCY REPORT NUMBER**

11. SUPPLEMENTARY NOTES The views expressed in this thesis are those of the author and do not reflect the official policy or position of the Department of Defense or the U.S. Government.

12a. DISTRIBUTION / AVAILABILITY STATEMENT Approved for public release. Distribution is unlimited.	**12b. DISTRIBUTION CODE** A

13. ABSTRACT (maximum 200 words)

This thesis will explore the hopping mobility approach for robotic vehicles used in Intra-Vehicular Activities (IVA) as an alternative mobility in space for small spacecraft equipped with robotic manipulators. A hopping maneuver uses the robotic manipulator to hop between two locations inside the host spacecraft. The maneuver is defined as three distinct phases: push, free-flying coast, and soft landing. Maneuvers such as hopping will be used to quickly move from one part of the host spacecraft to another, with little to no fuel consumption compared to zero-g climbing and propulsive free-flying.

This thesis answers the question, "Is there an ideal mobility for use in space that uses zero propellant?" The concept of an IVA hopping maneuver was explored, analyzed and experimentally demonstrated in simulation. Simulation results of such a maneuver validate hopping as a mobility approach in space. Future work includes ground testing of the hopping maneuver and implementation onboard the International Space Station to demonstrate an on orbit–hopping maneuver.

14. SUBJECT TERMS rendezvous, relative motion, proximity missions, formation flying, robotics, spacecraft, mobility in space, hopping	**15. NUMBER OF PAGES** 81
	16. PRICE CODE

17. SECURITY CLASSIFICATION OF REPORT	**18. SECURITY CLASSIFICATION OF THIS PAGE**	**19. SECURITY CLASSIFICATION OF ABSTRACT**	**20. LIMITATION OF ABSTRACT**
Unclassified	Unclassified	Unclassified	UU

NSN 7540-01-280-5500 Standard Form 298 (Rev. 2-89) Prescribed by ANSI Std. 239-18

THIS PAGE INTENTIONALLY LEFT BLANK

Approved for public release. Distribution is unlimited.

ROBOTIC SPACECRAFT HOPPING: APPLICATION AND ANALYSIS

Katrina P. Alsup
Lieutenant, United States Navy
BS, University of Washington, 2013

Submitted in partial fulfillment of the
requirements for the degree of

MASTER OF SCIENCE IN ASTRONAUTICAL ENGINEERING

from the

NAVAL POSTGRADUATE SCHOOL
December 2018

Approved by: Marcello Romano
Advisor

Josep Virgili-Llop
Co-Advisor

Garth V. Hobson
Chair, Department of Mechanical and Aerospace Engineering

THIS PAGE INTENTIONALLY LEFT BLANK

ABSTRACT

This thesis will explore the hopping mobility approach for robotic vehicles used in Intra-Vehicular Activities (IVA) as an alternative mobility in space for small spacecraft equipped with robotic manipulators. A hopping maneuver uses the robotic manipulator to hop between two locations inside the host spacecraft. The maneuver is defined as three distinct phases: push, free-flying coast, and soft landing. Maneuvers such as hopping will be used to quickly move from one part of the host spacecraft to another, with little to no fuel consumption compared to zero-g climbing and propulsive free-flying.

This thesis answers the question, “Is there an ideal mobility for use in space that uses zero propellant?” The concept of an IVA hopping maneuver was explored, analyzed and experimentally demonstrated in simulation. Simulation results of such a maneuver validate hopping as a mobility approach in space. Future work includes ground testing of the hopping maneuver and implementation onboard the International Space Station to demonstrate an on orbit–hopping maneuver.

THIS PAGE INTENTIONALLY LEFT BLANK

TABLE OF CONTENTS

LIST OF FIGURES

LIST OF TABLES

THIS PAGE INTENTIONALLY LEFT BLANK

LIST OF ACRONYMS AND ABBREVIATIONS

DOF	Degree of Freedom
ERA	European Robotic Arm
EVA	Extra-Vehicular Activity
GEO	Geosynchronous Earth Orbit
ISS	International Space Station
IVA	Inter-Vehicular Activity
JEM	Japanese Experiment Module
JEMRMS	Japanese Experiment Module Remote Manipulator System
LEO	Low Earth Orbit
LIDAR	Light Detection and Ranging
MBS	Mobile Base System
MSS	Mobile Servicing System
NASA	National Aeronautics and Space Administration
NPS	Naval Postgraduate School
S/C	Spacecraft
SERB	Space Experiments Review Board
SPDM	Special Purpose Dexterous Manipulator
SPHERES	Synchronized Position Hold, Engage, Reorient, Experimental Satellites
SRL	Spacecraft Robotics Laboratory
SRMS	Shuttle Remote Manipulator System
SSRMS	Space Station Remote Manipulator System

THIS PAGE INTENTIONALLY LEFT BLANK

ACKNOWLEDGMENTS

First, and foremost, I would like to thank Dr. Josep Virgili-Llop for your guidance and enthusiasm in my research project. I appreciate the countless hours you spent tutoring me and guiding my research to what is today. Words can't express how valuable your mentorship was on my academic career. Thank you.

I would next like to thank Jessica Shapiro, Justin Komma and additionally Jonathan Lang. From day one of this research project, through the ups and downs, you have been there to support me. Thank you for your support and constant encouragement day-in and day-out.

Next, I would like to thank, Dr. Marcello Romano. Thank you for accepting me to be a part of this team. The opportunity to work on this project was more than I ever dreamed of. Thank you.

Lastly, I want to recognize my family. You are my rock and my support through everything I do. Countless times I have called on each of you for your words of wisdom and sweet words of encouragement. Thank you all for being my biggest supporters. I am where I am because of you.

THIS PAGE INTENTIONALLY LEFT BLANK

I. INTRODUCTION

This thesis addresses the exploration of mobility in space and the versatility of robotic spacecraft in future space exploration. Robotics have been a cornerstone in space and will continue to be a vehicle for interplanetary mobility. Robotics provide a resilient platform that is able to operate in extreme environments where humans are not able to survive. The ability to operate in extreme temperatures makes robotics the ideal vessel to manipulate and adapt to the ever-changing environments that are present in interplanetary exploration.

Current mobility approaches for robotic vehicles in space can be categorized into two distinct approaches: 1) zero-g climbing and 2) propulsive free-flying. This thesis introduces hopping as an alternative mobility method for maneuvering of small spacecraft equipped with robotic manipulators. Mobility of such vehicles are the topic of on-going research in regards to on-orbit servicing of satellites, mining of planetary and asteroid bodies, space debris removal and construction of large apertures on-orbit. NASA has been exploring on-orbit servicing since 1973, when astronauts used a servicing vehicle to repair a heat shield (Ticker et al. 2015). The most prominent of the mission sets include, ETS-VII (Yoshida 2003), Orbital Express (Shoemaker and Wright 2004), and Canadarm (Sallaberger 1997). Hopping addresses the limitations of zero-g climbing and propulsive free-flying and provides an alternative propellantless mobility in space.

A. ZERO-G CLIMBING MOBILITY APPROACH

In a zero-g climbing approach, the spacecraft uses its robotic arms to transverse the host spacecraft by grasping onto the host spacecraft and moving between each location in a similar manner an astronaut would transverse in space. A humanoid robot was built by National Aeronautics and Space Administration's (NASA) Johnson Space Center. Robonaut 1 (Figure 1) consisted of two arms, two hands, one leg, and a camera for a head (Rehnmark et al. 2004). The robot would crawl outside the space station via the handrails that are used by astronauts to maneuver around the International Space Station (ISS) structure. The purpose of the robot was to operate in space and alleviate the maintenance

workload of astronauts by pairing with other robots to assist the astronauts during space walks (Ambrose et al. 2000). This zero-g climbing approach is slow (1.016 cm/s) and limited in its capability due to the need of specialized handrails for the Robonaut hands to grasp and the limited number of handrails available around the exterior of the space station (Rehnmark et al. 2004). Robonaut 2 was launched to the ISS in February 2011 (Ambrose et al. 2000). The updated Robonaut 2 (Figure 2) added an additional leg to Robonaut 1 as well as additional sensors and faster maneuverability times with a limb speed of 2 m/s (NASA, 2018).

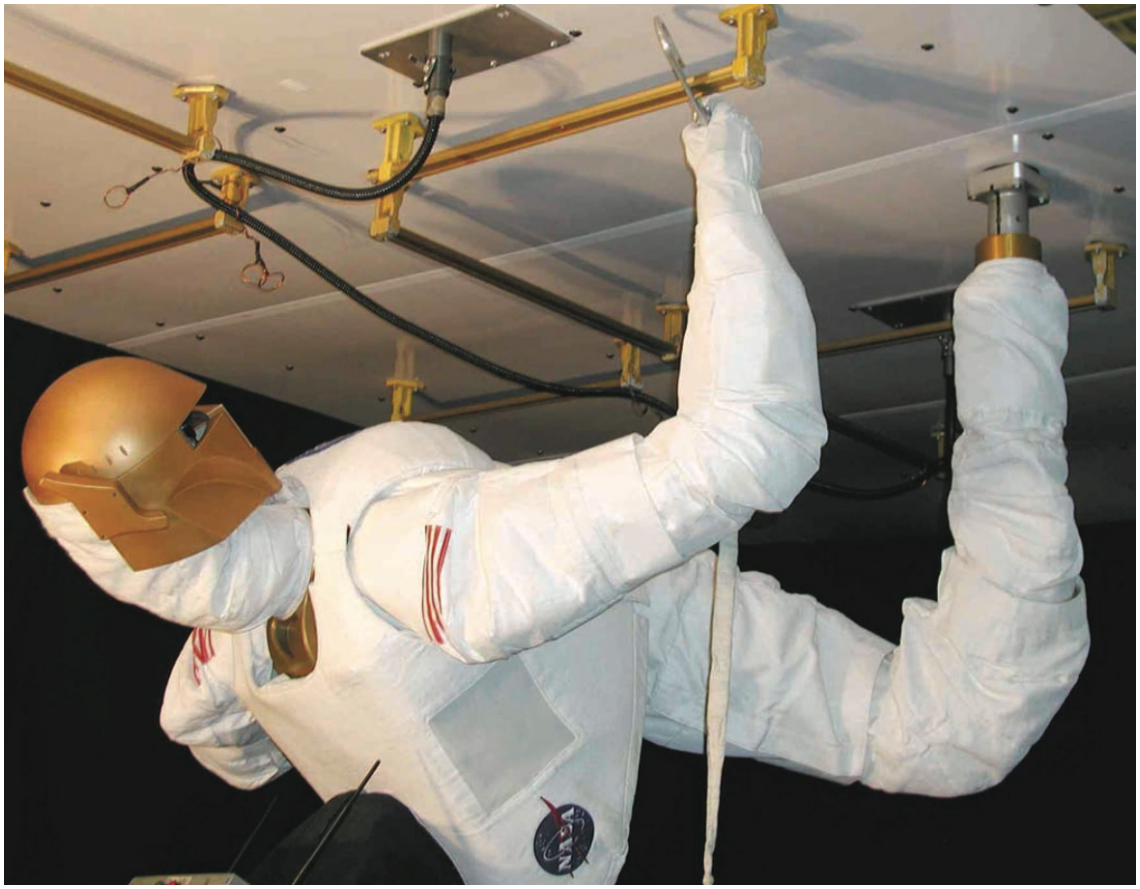

Figure 1. Robonaut 1. Source: Rehnmark et al. (2004).

Figure 2. Robonaut 2. Source: NASA (2018).

The limitation of zero-g climbing mobility approach is the dependence on constant contact with the host spacecraft structure. To maneuver from one side of the host spacecraft to the other would require climbing the perimeter of the host spacecraft. This movement is slow in a translational direction along the edges of host structure and is limited to regions of the host spacecraft where there are specialized handrails installed.

B. PROPULSIVE FREE-FLYING MOBILITY APPROACH

The propulsive free-flying mobility approach enables spacecraft to maneuverer quickly in space. In this alternative approach, the spacecraft utilizes the limited supply of propellant carried onboard to move from one location to the next using onboard guidance and navigation systems. One example of an external propulsive free-flying approach can be found in the Autonomous Extravehicular Robotic Camera (AERCam) (Figure 3), developed by NASA. AERCam was a free-flyer spacecraft tested in 1997 as a remote camera capable of inspection of the external surfaces of the ISS (Chen et al. 2013). Designed for external use, the propellant onboard provides the only fuel to maneuver the spacecraft.

Figure 3. AERCam. Source: Chen et al. (2013).

The Japanese Space Agency created Internal Ball Camera (Int-Ball) (Figure 4), is another example of a propulsive free-flyer for similar observatory uses internal to the ISS. The small free-flyer is capable of capturing images previously unable to be captured by astronauts due to the location of the wall mounted cameras onboard the ISS (Japan

Aerospace Exploration Agency, 2017). Int-ball reduces the time requirements of the astronauts to do the simple task of taking photos or videos thus freeing up the crew's time to conduct other experiments. As a free-flyer, the robot moves autonomously to predetermined positions for capturing images and videos with the intention of eliminating crew involvement in such activities. Unlike the AERCam, Int-ball is exclusively used for internal observations and, as such, has the added environment of air flow inside the ISS.

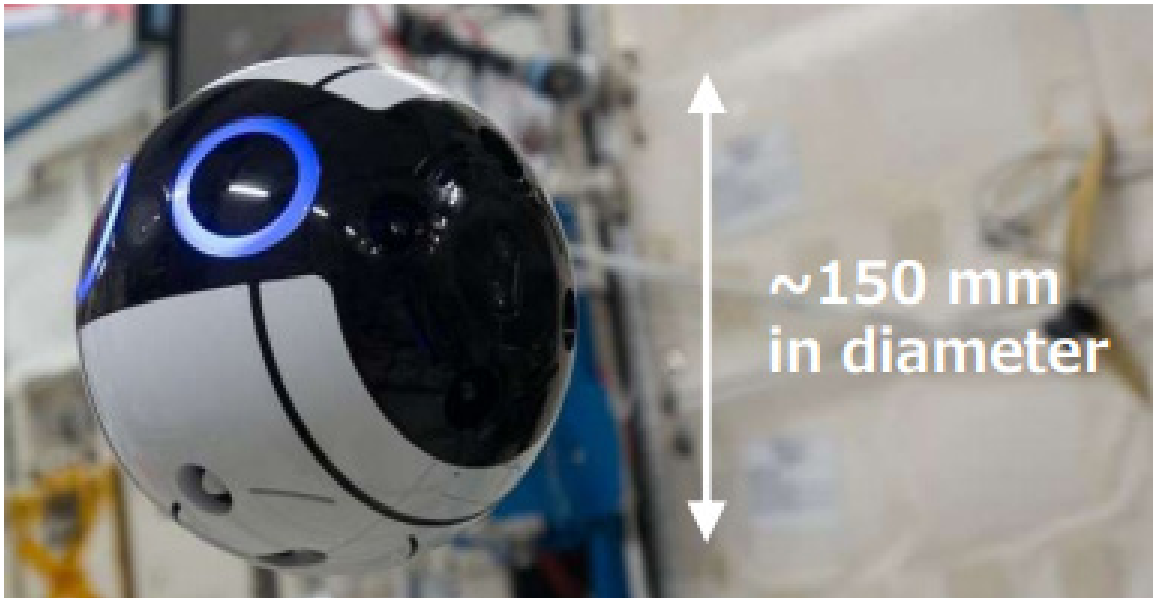

Figure 4. JAXA Int-Ball. Source: Japan Aerospace Exploration Agency (2017).

In addition to these free-flyers, other robotic spacecraft assist astronauts in routine tasks and gather multimedia data via their onboard sensors. A new addition onboard the ISS, the Crew Interactive MObile companioN (Cimon) is an experiment developed to assist astronauts in maintenance, experimentation, and motor skills with the added capability of access to saved files via voice commands (NASA, 2018). As the program comes online, more information will be available on the value Cimon may have on assisting the crew.

The free-flying mobility approach is versatile and has the ability to maneuver quickly. The limitations of such robotic spacecraft is the limited fuel onboard. Once the fuel supply has been depleted, the spacecraft must be refueled to continue mission tasking.

The mission tasking has to be prioritized based on the available fuel remaining, which limits the capabilities of mission the robotic vehicle can perform.

C. ROBOTIC MANIPULATORS

Robotic manipulators have expanded the capability of structures built in space and reduced the risk to astronauts by limiting EVA. The length of the robotic manipulators extends the reach that would be achievable by an astronaut alone. Robotic manipulators enhance the capabilities of robotic spacecraft and in terms of mobility, create a sub-category to be explored in regards to mobility in space.

Canada has contributed multiple systems in support of furthering mobility in space, in particular modifications to the Shuttle and ISS. The collection of robotic systems developed by Canada is the Mobile Servicing System (MSS)(Figure 5), which includes the Mobile Base System (MBS), the Space Station Remote Manipulator System (SSRMS), and the Special Purpose Dexterous Manipulator (SPDM). Not included in the MSS onboard the ISS is the Shuttle Remote Manipulator System (SRMS) or Canadarm for short is yet another contribution to space robotic manipulators by Canada. The Canadarm is 15 meters in length with six joints to support Space Shuttle operations (Sallaberger 1997 pg 240). The SSRMS or Canadarm2 is 17.1 meters in length with seven joints to support Space Station operations (Sallaberger 1997, pg 41). Special Purpose Dexterous manipulator (SPDM) or Dextre is two meters in length for each arm with seven joints in each arm and the ability to conduct a degree of freedom with a body roll was built to support ISS operations (Sallaberger 1997, pg 241) seen in Figure 6. Advances in robotics have enabled the continued development of large structures in space. The long reach of the robotic manipulator help astronauts assemble structures in space with minimal mobility on the part of the astronaut. Safety of the astronauts in space is a top priority and a way to decrease the risk includes minimizing astronaut EVA.

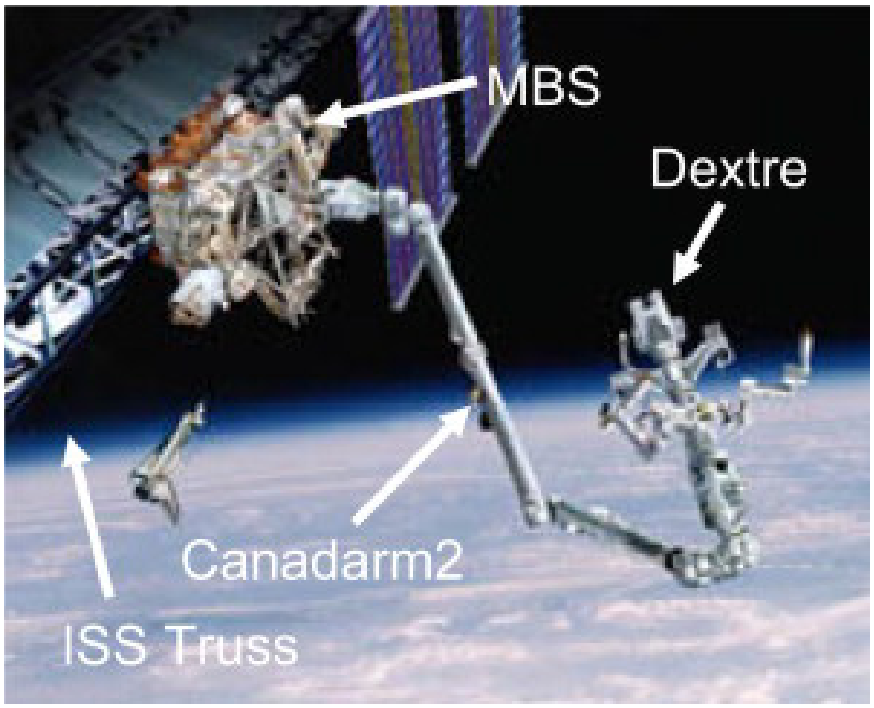

Figure 5. Artist Rendition of Dextre Attached to Canadarm2 Operating from the Mobile Base System on ISS. Source: Coleshill et al. (2009).

Figure 6. Artist Rendition of Dextre. Source: Coleshill et al. (2009).

Canada was not the only contributor of a robotic arm to the ISS. The Japanese Experiment Module (JEM) Remote Manipulator System (JEMRMS) and the European Robotic Arm (ERA) were both robotic arms to the ISS. Table 1 provides a side-by-side comparison of the three robotic arms developed for the ISS.

Table 1. Comparative Study of SSRMS, JEMRMS and ERA.
Source: Adopted from Patten et al. (2002).

	SSRMS	**JEMRMS (MA)**	**ERA**
SPAN	14.22 m	9.91 m	11.3 m
Boom Span	7.11 m	3.93 m and 3.94 m	7.77 m
DOF's	7	6	7
Joints	Offset	Offset	Inline
Base	Relocatable	Fixed	Relocatable
Mass	1336 kg	757 kg	630 kg
Max Holding Capacity	116,000 kg	7,000 kg	8,000 kg
Translation (at max capacity)	12 mm/sec	20 mm/sec	10 mm/sec
Rotation (at max capacity)	0.04 deg/sec	0.5 deg/sec	0.15 deg/sec

Developed by National Space Development Agency of Japan (NASDA) Engineering Test Satellite VII (ETS-VII) demonstrated on-orbit capabilities with a 2-meter-long arm and six degrees of freedom (DOF) manipulator mounted on a host spacecraft. The objective of the on-orbit testing was to demonstrate the ability of rendezvous, docking and on-orbit servicing. The objective of this experiment extended to the concept of a manipulator moving without disturbing the base-spacecraft.

The limitation of robotic manipulators is the reliance of humans in the loop. The astronauts require precision maneuvers and, thus, require extensive training on each of the robotic systems and their respective manipulators.

D. THE HOPPING MOBILITY APPROACH

Mobility in space is limited in both speed and fuel consumption. A hopping maneuver is a new mobility approach that alleviates the limitations of zero-g climbing approach (speed) and free-flyer (limited propellant) and the human in the loop requirement that current robotic manipulators in space require. A hopping mobility approach is defined when a spacecraft uses the forces applied by the manipulator to push-off and "jump" between two locations. A hopping maneuver is comprised of three phases: push, free-flying coast, and a soft-landing at the final location. This maneuver has the potential to be propellantless and faster than existing mobility approaches.

This thesis will address the question, is there an ideal mobility for use in space that uses zero propellant? A hopping mobility approach is introduced as a potential alternative mobility approach to zero-g climbing and free-flying for robotic spacecraft equipped with a robotic manipulator. Spacecraft equipped with a robotic arm provide a versatility for a wide range of space missions including servicing other spacecraft, assembly of large structures, removal of orbital debris and assisting astronauts with routine tasks.

Hopping maneuvers are not a new field of study but rather have been extensively researched for planetary exploration by Burdick's "Minimalist Jumping Robotics for celestial Exploration," Ulamec's "Hopper Concepts for Small Body Landers," and Hockman's "Stochastic Motion Planning for Hopping Rovers on Small Solar System Bodies" to name a few. The concept focused on exploiting the gravity or lack of gravity on other planets and how a hopping mobility approach could speed up travel time by covering much larger distances in shorter amounts of time. Additionally, other planets have vastly different terrains that typical travel on wheels might be difficult to travel on, hopping would alleviate this difficulty. The concept of hopping does not need to be limited to terrestrial mobility but is researched in this thesis as a means of mobility in space, utilizing the same concept of exploiting the lack of gravity to the advantage of the vehicle. To demonstrate

the hopping maneuver presented in this thesis, the Astrobee free-flyer developed by NASA - Ames Research Center will be utilized as a platform to demonstrate the mobility approach. Using the components installed on Astrobee, software was developed to exploit and utilizes the onboard components to maneuver Astrobee propellantlessly.

E. EVOLUTION OF THE ASTROBEE PROJECT

The Astrobee free-flyer is a robotic spacecraft developed as a platform for guest scientist research onboard the ISS. The Astrobee robotic spacecraft is an evolutionary project that originated with the Synchronized Position Hold Engage and Reorient Experiment Satellites (SPHERES).

1. Astrobee's Precursor: SPHERES

SPHERES is a product of the MIT Space Systems Laboratory delivered by NASA mission Expedition 8 to the ISS and remains an active experiment onboard. SPHERES (Figure 7) consists of three free-flying robotic spacecraft, provide an educational platform for researchers to test navigation, maneuvering, and guidance control implementation on multiple spacecraft simultaneously (McCamish et al. 2009). Shaped like spheres, these satellites fly inside the ISS and test autonomous rendezvous and docking maneuvers. The SPHERES research platform laid the groundwork for the next generation of robotics in space like NASA's free-flyer, Astrobee (NASA, International Space Station Basics).

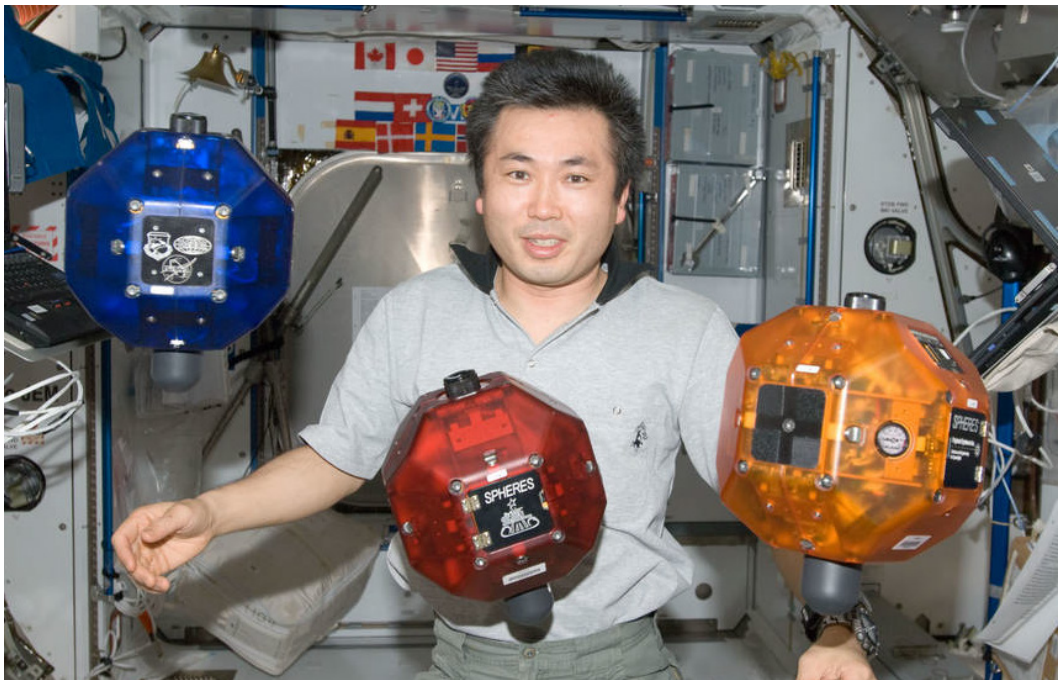

Figure 7. SPHERES Experiment inside the ISS. Source: NASA, SPHERES (2017).

SPHERES requires constant astronaut supervision during all experiments. Astrobee will serve as the replacement to SPHERES and builds off many of the same features as AERCam and PSA in respect to free-flying capabilities. Due to the autonomous free-flying ability that Astrobee is projected to have, will require little to no astronaut supervisor which would alleviate the consuming time demands of the SPHERES experiments (Smith et al. 2016).

2. Astrobee Anatomy

Astrobee is a free-flying autonomous robot designed for Inter-Vehicular Activity (IVA) inside the ISS. The basic components of Astrobee are identified in Figure 8. The mechanical arm pictured is the manipulator developed by the NASA team. NPS colleagues are researching a more dexterous manipulator for Astrobee but the software for this thesis was developed with initial NASA manipulator arm.

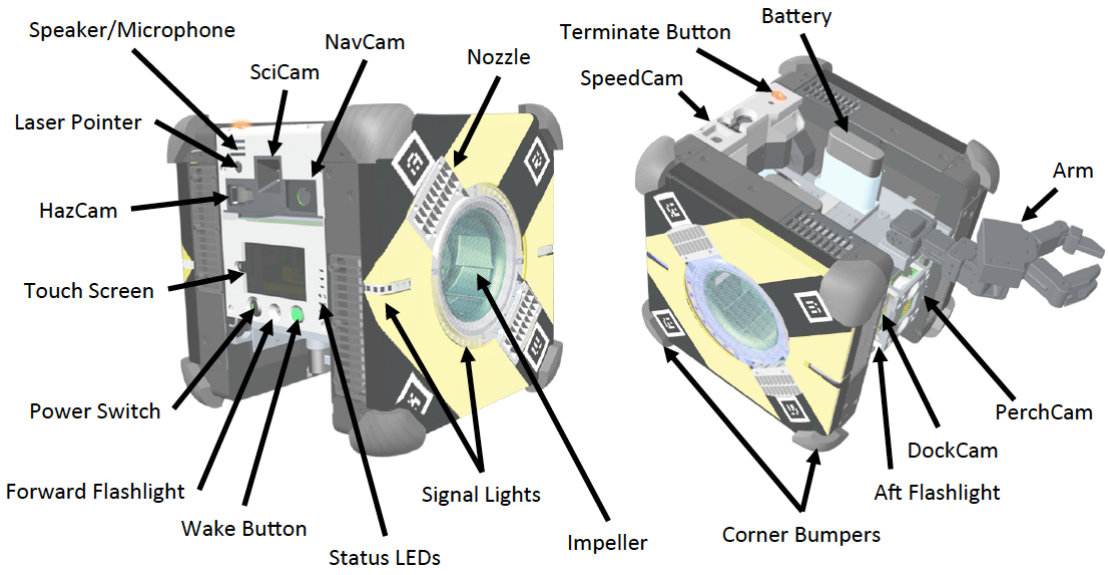

Figure 8. Astrobee Anatomy. Source: NASA (2017).

3. Astrobee's Current Mission Capabilities

The current mission capability for Astrobee is to use its manipulator arm to perch itself. Astrobee has installed fans to propel and stabilize itself. Each unit is equipped with camera for experiment observations and Light Detection and Ranging (LIDAR) features to enable the vehicle to maneuver throughout the space station (autonomously) (Smith et al. 2016). From the perched position, the camera can focus on the astronauts during scientific research and testing. Astronauts can maneuver the spacecraft to any handrail that would be best for viewing the experiment. The range of motion of the manipulator arms suggests that Astrobee could actuate the manipulator over the range to ramp up the velocity on the joints and push itself from handrail to handrail.

F. PREVIOUS WORK

This thesis is a continuation of previous work done by Naval Postgraduate School (NPS) thesis student Andrew Bradstreet, whose thesis work explored the study of a push and planar hopping maneuver of robots (Bradstreet 2018). The platform for this planar hopping maneuver was Manipulator Satellite (ManiSat), the Spacecraft Robotics Laboratory's (SRL's) Floating Spacecraft Simulator (FSS). Bradstreet performed both

simulations and hardware testing on the SRL's test-bed, Proximity Operation of Spacecraft: Experimental hardware-In-the-loop Dynamic Simulator (POSEIDYN). The goal of his experiments was to prove the feasibility of a propellantless push/catch maneuver. ManiSat, performed a self-toss from the left handrail with the direction of motion to the right handrail as pictured in Figure 9. The floating robot entered a free-flying coast upon the gripper's release of the handrail until ManiSat reached the opposite handrail, at which time executed a soft-landing. The results of the experiment validate the hopping maneuver and its ability to propellantlessly maneuver a spacecraft.

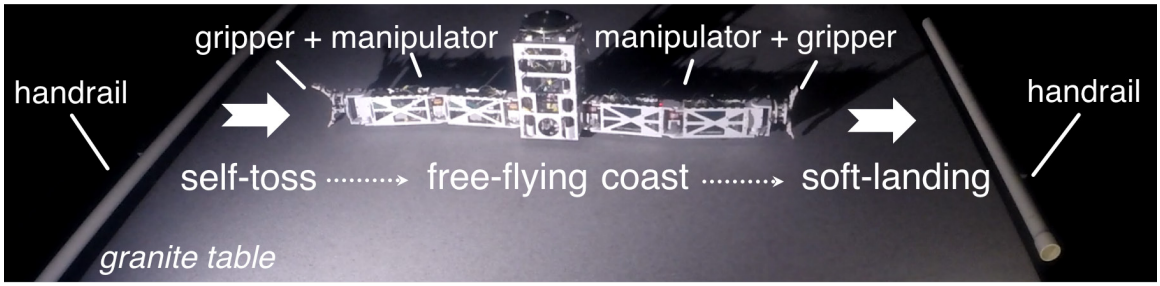

Figure 9. Experimental Demonstration of a Hopping Maneuver at the NPS Planar Air Bearing Test-Bed. Source: Bradstreet (2017).

G. THESIS OVERVIEW

This unique hopping maneuver, developed at NPS, will be the first on-orbit demonstration of a non-traditional maneuver approach. This thesis will cover both the theory and formulation of the control algorithms used and the implementation of the controllers. The following chapters will outline the development, simulation, testing, and concept of operations for an on-orbit demonstrations of the hopping maneuver of NASA - Ames Research Center's free-flyer, Astrobee. Chapter II provides formulation of the general hooping mobility approach. Chapter III explains in detail the simulation experiments. Chapter IV will present the results of the experiments. Chapter V will explain the implementation of the hopping maneuver onboard the ISS and provide a detailed concept of operation for the ISS experiments. Chapter VI will be all conclusions from this thesis.

THIS PAGE INTENTIONALLY LEFT BLANK

II. IVA ROBOTIC SPACECRAFT HOPPING

Here the equation of motion formulation and guidance strategy for an IVA hopping maneuver is presented in detail. To help in the formulation, the maneuver divides into three phases: push, free-flying coast, and soft-landing. Each phase outlines in detail with the governing equations derived therein for the general case of a hopping maneuver.

A. HOPPING: A THREE-PHASED MANEUVER

A spacecraft hopping maneuver is conceptually divided into three phases in which a robotic vehicle hops between two locations on the host spacecraft. Phase one of a hopping maneuver is a push motion, in which the hopping spacecraft uses its robotic manipulator to exert a motion against the host spacecraft, propelling the hopping spacecraft towards its final destination. At the time the gripper releases the handrail, the hopping spacecraft enters phase two, called the free-flying coast phase. The final phase of a hopping maneuver is the soft landing of the hopping spacecraft at the desired end location. Figure 10 illustrates conceptual division into three phases.

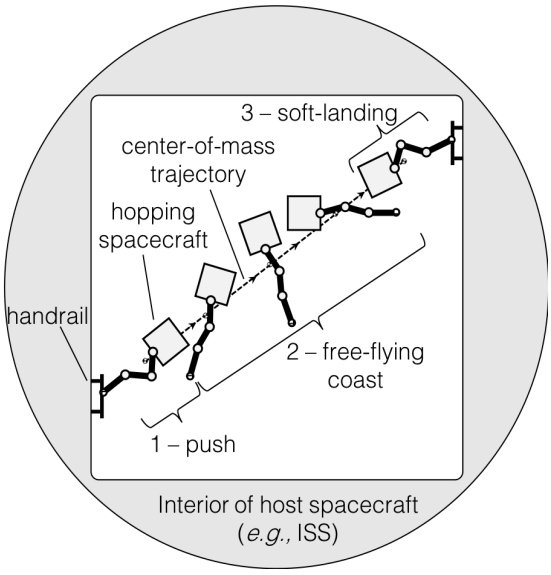

Figure 10. Schematic of Maneuver.

B. FORMULATION

The governing equations for each phase are here derived. To do so, the following assumptions are made:

- The robotic vehicle consists of multiple rigid body systems moving in three-dimensional space.
- Relative orbital dynamic effects are negligible due to the close proximity of the hopping spacecraft to the host spacecraft.
- All properties (state and inertia) of the hopping robotic vehicle are known.
- Ideal contact dynamics exist between the hopping vehicle and the host spacecraft.

1. Equations of Motion of a Free-Flying Robotic Multibody System

The generalized coordinates of the base-spacecraft are position ($\boldsymbol{r}_0$) and orientation ($\boldsymbol{\theta}_0$) as written in Equation 1.

$$\boldsymbol{q_0} = \begin{bmatrix} \boldsymbol{r_0} \\ \boldsymbol{\theta_0} \end{bmatrix} \tag{1}$$

The generalized joint positions for a manipulator of the multibody system are written in Equation 2, where N denotes the number of joints.

$$\boldsymbol{q_m} = \begin{bmatrix} \boldsymbol{q_1} \\ \boldsymbol{q_2} \\ \vdots \\ \boldsymbol{q_{N-1}} \\ \boldsymbol{q_N} \end{bmatrix} \tag{2}$$

Thus the position and orientation of the multibody system is given by $\boldsymbol{q}$ as written in Equation 3.

$$\boldsymbol{q} = \begin{bmatrix} \boldsymbol{q_0} \\ \boldsymbol{q_m} \end{bmatrix} \tag{3}$$

The velocities and accelerations are written as Equations 4 and 5.

$$\dot{\boldsymbol{q}} = \begin{bmatrix} \dot{\boldsymbol{q}}_0 \\ \dot{\boldsymbol{q}}_m \end{bmatrix} \tag{4}$$

$$\ddot{\boldsymbol{q}} = \begin{bmatrix} \ddot{\boldsymbol{q}}_0 \\ \ddot{\boldsymbol{q}}_m \end{bmatrix} \tag{5}$$

The hopping maneuver for a multibody system can be represented by the generalized equations of motion (Dubowsky et al. 1993) written as Equation 6:

$$\boldsymbol{H}\ddot{\boldsymbol{q}} + \boldsymbol{C}\dot{\boldsymbol{q}} = \boldsymbol{\tau} \tag{6}$$

where $\boldsymbol{\tau}$ is the generalized torques. The generalized inertia matrix $\boldsymbol{H}$ is a function of $\boldsymbol{q}$ for the multibody system. The generalized convective inertia matrix of the system is $\boldsymbol{C}$ and is a function of $\boldsymbol{q}$ and $\dot{\boldsymbol{q}}$ of the base and joints. Equation 6 can therefore be defined by subscript notation 0 for the base-spacecraft and subscript m for the manipulator as is written in Equation 7:

$$\begin{bmatrix} \boldsymbol{H}_0 & \boldsymbol{H}_{0m} \\ \boldsymbol{H}_{0m}^T & \boldsymbol{H}_m \end{bmatrix} \begin{bmatrix} \ddot{\boldsymbol{q}}_0 \\ \ddot{\boldsymbol{q}}_m \end{bmatrix} + \begin{bmatrix} \boldsymbol{C}_0 & \boldsymbol{C}_{0m} \\ \boldsymbol{C}_{m0} & \boldsymbol{C}_m \end{bmatrix} \begin{bmatrix} \dot{\boldsymbol{q}}_0 \\ \dot{\boldsymbol{q}}_m \end{bmatrix} = \begin{bmatrix} \boldsymbol{\tau}_0 \\ \boldsymbol{\tau}_m \end{bmatrix} \tag{7}$$

Matrices $\boldsymbol{H}$ and $\boldsymbol{C}$ can be computed via SRL's SPAcecraft Robotics Toolkit (SPART) software (Virgili-Llop et al. 2018). This software inputs a user defined robot with all its corresponding parameters and generates the robot model, Jacobians, inertia matrices $\boldsymbol{H}$, and convective inertia matrices $\boldsymbol{C}$.

The momenta $\boldsymbol{\mathcal{M}}$ of the system including the linear ($\mathcal{P}$) and angular momenta ($\mathcal{L}$) are expressed by the following equations:

$$\boldsymbol{\mathcal{M}} = \begin{bmatrix} \boldsymbol{\mathcal{L}} \\ \boldsymbol{\mathcal{P}} \end{bmatrix} = \boldsymbol{H}_0\dot{\boldsymbol{q}}_0 + \boldsymbol{H}_{0m}\dot{\boldsymbol{q}}_m \tag{8}$$

$$\frac{d\boldsymbol{\mathcal{M}}}{dt} = \boldsymbol{\tau}_0 \tag{9}$$

The Jacobian, **J** maps generalized joint-space velocities $\dot{\boldsymbol{q}}$ to task-space velocities $\boldsymbol{t}_P$ and is required to adequately control the system (Siciliano et al. 2010).

$$\boldsymbol{t}_P = \boldsymbol{J}_P\dot{\boldsymbol{q}} = \begin{bmatrix} \boldsymbol{J}_{0,P}, & \boldsymbol{J}_{M,P} \end{bmatrix} \begin{bmatrix} \dot{\boldsymbol{q}}_0 \\ \dot{\boldsymbol{q}}_m \end{bmatrix} \tag{10}$$

$$\boldsymbol{t}_P = \begin{bmatrix} \dot{\boldsymbol{r}}_P \\ \boldsymbol{\omega}_P \end{bmatrix} \tag{11}$$

The Jacobian describes the motion of the end-effector based on the rotation of the manipulator joints results with a change in attitude and position of the base (Wilde et at. 2018).

2. Equations of Motion During the Push

A hopping maneuver begins with the robotic spacecraft attached to the handrail in what is called a perched mode. This is both a stationary position and the starting position of the hopping maneuver. From the perched position, the robotic spacecraft is rigidly attached to the handrail. The manipulator attached to the hopping spacecraft provide three degrees of freedom to orient the vehicle towards its desired final destination.

The push is the initial motion of the hopping mobility approach. From the perched position, the robotic spacecraft's gripper is attached to the handrail while the manipulator joints are actuated. The end-effector maintains rigid connection with the host spacecraft and the mapping between joint velocities and the end-effector velocities are expressed:

$$\boldsymbol{t_e = 0 = J_{0,E}\dot{q}_0 + J_{m,E}\dot{q}_m} \quad \textit{(12)}$$

$$\boldsymbol{t_e = 0 = J_{0,E}u_0 + J_{m,E}u_m} \quad \textit{(13)}$$

the resulting velocities of the base-spacecraft during the push are obtained as follows:

$$\boldsymbol{\dot{q}_0 = -J_{0,E}^{-1}J_{m,E}\dot{q}_m} \quad \textit{(14)}$$

Upon the completion of the push, the gripper releases propelling the hopping spacecraft in the oriented direction and exploits a desired linear and angular velocity of the hopping vehicle to reach the final destination. The momenta of the system during the push is as follows:

$$\boldsymbol{\mathcal{M} = \left(H_{0m} - H_0 J_{0,E}^{-1} J_{m,E}\right)\dot{q}_m} \quad \textit{(15)}$$

3. Equations of Motion During the Free-Flying Coast

The moment the gripper releases the handrail, the free-flying coast phase of the hopping maneuver begins. If no forces are applied to the multibody system then the

momenta of the system is constant and the governing equations of the multibody system are as follows:

$$\boldsymbol{\tau_0 = 0} \tag{16}$$

$$\boldsymbol{\mathcal{M} \rightarrow constant} \tag{17}$$

$$\boldsymbol{\dot{r}_c = \frac{\mathcal{P}}{m_{tot}} \rightarrow constant} \tag{18}$$

The velocity of the base is, in general, not constant (as $\boldsymbol{H}_0$ is a function of $\boldsymbol{q}$ and thus changes with orientation, $\boldsymbol{\theta}$)

$$\boldsymbol{\dot{q}_0 = H_0^{-1}(\mathcal{M} - H_{0m}\dot{q}_m)} \tag{19}$$

If propulsion is used during the free-flying phase, the momenta would no longer be conserved. This part of the phase does have the option of using onboard propulsion to produce mid-course corrections as needed but the equations of motion during the free-flying coast were formulated without the use of the propulsion system. Errors may derive from imperfect release conditions during the push from the handrail. These errors can be corrected by modifying the translational trajectory to achieve the initial desired end location

4. Equations of Motion During the Landing

The soft-landing ends the maneuver when the gripper grasps the handrail with a zero relative velocity between the arm and the stationary handrail of the host spacecraft.

$$\boldsymbol{t_e = 0 = J_{0,E}\dot{q}_0 + J_{m,E}\dot{q}_m} \tag{20}$$

With $\dot{\boldsymbol{q}}_0$ defined from Equation 18 and t_e from Equation 19, $\dot{\boldsymbol{q}}_m$ is as follows:

$$\boldsymbol{\dot{q}_m = \left(J_{0,E}H_0^{-1}H_{0m} - J_{m,E}\right)^{-1}\left(J_{0,E}H_0^{-1}\mathcal{M}\right)} \tag{21}$$

The movement of the arm to counter the rotation of the hopping spacecraft is desired to catch the handrail with a relative zero velocity between the stationary host handrail and the hopping spacecraft.

The free-fly coast phase is further categorized into two categories, a passive phase and an active phase. The second phase of the free-flying coast maneuver is known as the active phase due to the active moving of the manipulator with respect to the hopping vehicle during the coast. Due to the moving of the manipulator $\dot{\boldsymbol{q}}_0$ changes throughout this phase of the maneuver. The second phase of the free-flying coast maneuver is the beginning of the soft-landing maneuver.

C. PLANNING A HOPPING MANEUVER

Figure 11 notionally shows the geometric definition of a hopping maneuver. All vectors are projected onto the inertial Cartesian Coordinate System.

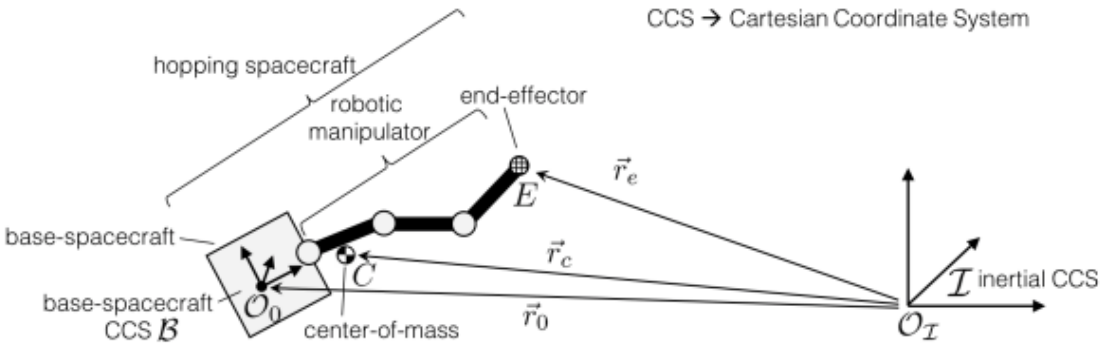

Figure 11. Hopping Spacecraft Definitions.

The problem formulation consists of both direct and inverse hopping problems. The direct formulation consists of solving for the trajectory once the generalized variables are known. The inverse formulation consists of solving for the trajectory given specified hopping inputs *i.e.*, start and end locations.

1. Direct Hopping Problem

In the direct hopping problem, the generalized variables of the multibody system are known. Given that the position, $\boldsymbol{r}_e$ and the orientation $\boldsymbol{\theta}_e$ of the end-effector and the $\boldsymbol{q}$ of the system are known, then the kinematics can be solved for, providing the trajectory of the hopping maneuver.

For the push, Equation 22 holds true.

$$\begin{bmatrix} \boldsymbol{r_e} \\ \boldsymbol{\theta_e} \end{bmatrix} \rightarrow \boldsymbol{constant} \tag{22}$$

During this phase, $\dot{\boldsymbol{q}}_m$ is a controlled input. Note that the manipulator is velocity-controlled, thus the configuration at any time during the hopping maneuver is simply the integration of $\dot{\boldsymbol{q}}_m$. At the time of release, the manipulator configuration, $\boldsymbol{q}_m$ and manipulator velocity $\dot{\boldsymbol{q}}_m$ are therefore known. Using Equation 14, the momenta of the system can be computed.

For the free-flying coast, the center-of-mass is constant (Equation 17). The manipulator is assumed to be fixed during the initial free-flying coast and thus the base-spacecraft velocity, $\dot{\boldsymbol{q}}_0$ can be solved for with Equation 18. The trajectory is thus solved for by integrating $\dot{\boldsymbol{q}}_0$ to get the $\boldsymbol{q}_0$ (position and orientation) of the base-spacecraft over the course of the free-flying coast phase of the hopping maneuver.

During the soft-landing, the manipulator velocity ($\dot{\boldsymbol{q}}_m$) is as written in Equation 23 until the end-effector grasps the destination handrail, at which time, the base-spacecraft velocity ($\dot{\boldsymbol{q}}_0$) will obey Equation 24.

$$\dot{\boldsymbol{q}}_{\boldsymbol{m}} = \left(\boldsymbol{J}_{\boldsymbol{0,E}}\boldsymbol{H}_{\boldsymbol{0}}^{-\boldsymbol{1}}\boldsymbol{H}_{\boldsymbol{0m}} - \boldsymbol{J}_{\boldsymbol{m,E}}\right)^{-\boldsymbol{1}}\left(\boldsymbol{J}_{\boldsymbol{0,E}}\boldsymbol{H}_{\boldsymbol{0}}^{-\boldsymbol{1}}\boldsymbol{\mathcal{M}}\right) \tag{23}$$

$$\dot{\boldsymbol{q}}_{\boldsymbol{0}} = -\boldsymbol{J}_{\boldsymbol{0,E}}^{-\boldsymbol{1}}\boldsymbol{J}_{\boldsymbol{m,E}}\dot{\boldsymbol{q}}_{\boldsymbol{m}} \tag{24}$$

The goal of a soft-landing is to have the difference between the free-flying coast velocity (Equation 18) and the velocity of the base-spacecraft (Equation 24) following the moment the end-effector grips the destination handrail to be zero.

Once the base-spacecraft is grasping the final handrail, $\dot{\boldsymbol{q}}_m$ goes to zero after which time, the hopping maneuver is complete.

2. Inverse Hopping Problem

In the inverse hopping problem, the initial position, $\boldsymbol{q}_0$ of the hopping spacecraft is known. The corresponding release configuration of the manipulator needs to be solved

for. The inverse hopping maneuver takes a range of kinematic solutions found from the direct hopping problem and correlates the hopping spacecraft's current height with the closest height data point to get the corresponding release configuration of the manipulator.

D. CONCLUSION

A planar hopping maneuver is feasible with small spacecraft equipped with a robotic manipulator. This simple hopping maneuver is constructed in such a way that the only control variable is the point of release determined by the orientation of the manipulator. The limited factor in the hopping maneuver therefore is the range of motion the manipulator is capable of (DOF).

III. SIMULATED HOPPING MANEUVERS WITH THE ASTROBEE FREE-FLYER

To showcase and verify the proposed mobility approach, the Astrobee free-flyer is used for simulation of the hopping maneuver inside the simulated ISS. With the current hardware installed on the robot, Astrobee could perform a hopping maneuver by actuating joints in the manipulator to hop between two locations. The range of the manipulator and the velocities the joints, create a platform to conduct IVA hopping without additional hardware; merely a software upgrade could make Astrobee the first robotic spacecraft to hop in space. Results of the hopping maneuver simulate the inside of the ISS.

The goal is for Astrobee to start from a perched configuration on an ISS handrail and push itself off the handrail, free-fly coast across the space station, and catch itself via a soft-landing. The simulated hopping maneuver provides proof of concept for ground test experiments as well as the ISS experiment. The data collected in the simulated environment will in future work be compared with ground tests to validate the correct forces and ultimately to provide validation to the experiment for safety purposes prior to the ISS experiment.

A. ASTROBEE

NASA – Ames' free-flyer robot, Astrobee is an available platform to conduct control algorithms through the available guest scientist research program put forth by NASA. The hopping mobility approach of this thesis, commonly called astrobatics due to the gymnastic characterizes of the backflip involved in the maneuver is a software only payload that can be uploaded to the free-flyer while in the ISS. Prior to conducting experiments onboard the ISS, simulated and ground testing must first demonstrate the feasibility of the maneuver and demonstrate the hopping maneuver is safe for testing in the ISS.

The simulated planar Astrobee experiment consists of a base spacecraft and six manipulator links. The six joint positions of Astrobee's manipulator are written in Equation 25, named in Table 2 and the associated links are displayed in Figures 12 and 13.

$$q_m = \begin{bmatrix} q_1 \\ q_2 \\ q_3 \\ q_4 \\ q_5 \\ q_6 \end{bmatrix} \tag{25}$$

Table 2. Name Association for the Six Joint Positions of Astrobee. Source: NASA (2018).

Joint	q_m
Arm Proximal	q_1
Arm Distal	q_2
Gripper Left Proximal	q_3
Gripper Left Distal	q_4
Gripper Right Proximal	q_5
Gripper Right Distal	q_6

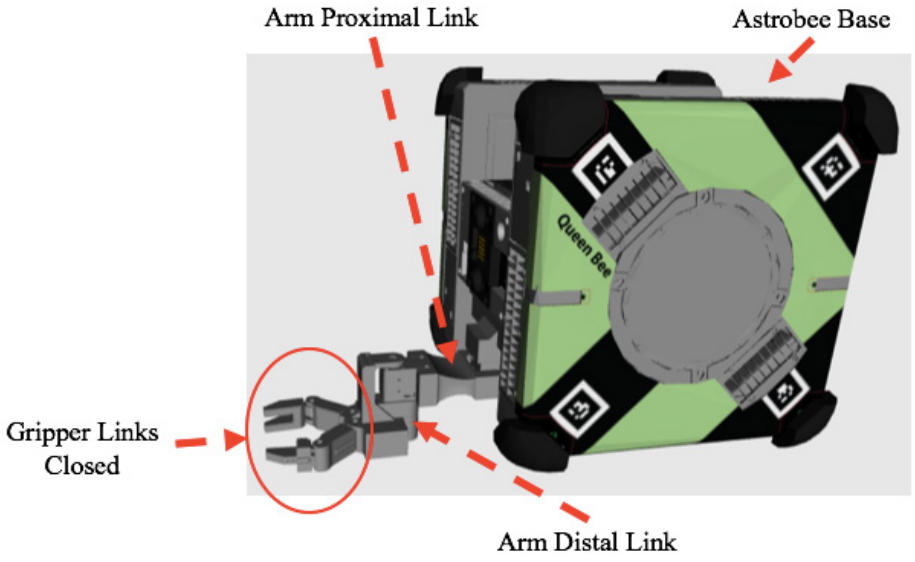

Figure 12. Named Links of Astrobee from Side View.

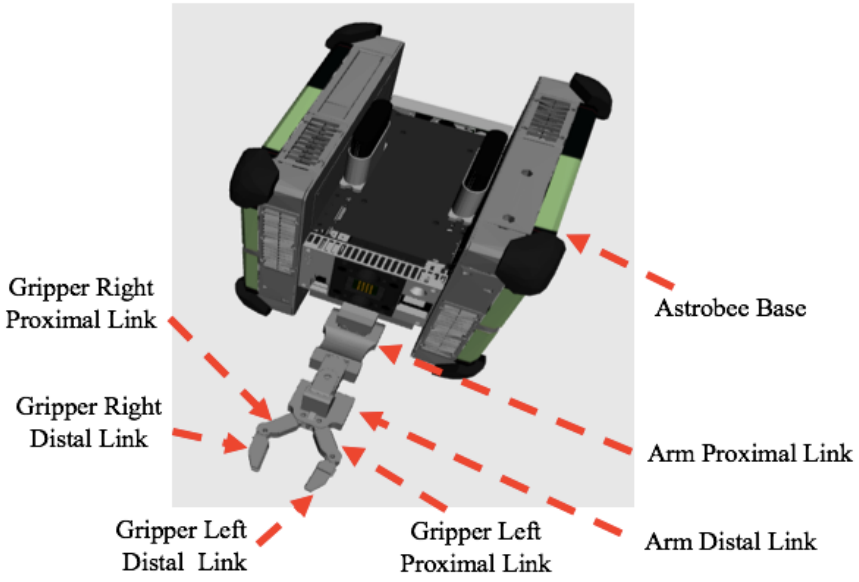

Figure 13. Named Links of Astrobee from Bottom View.

The joints q_3 through q_6 make up the gripper and are grouped together as such to be open or closed as needed for launch and landing.

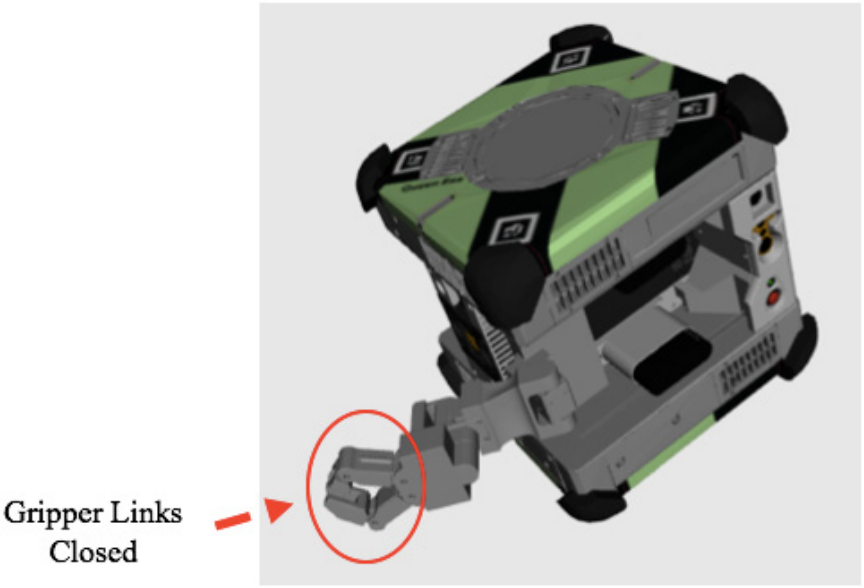

Figure 14. Gripper Links in the Closed Position with Astrobee in the Perch Configuration.

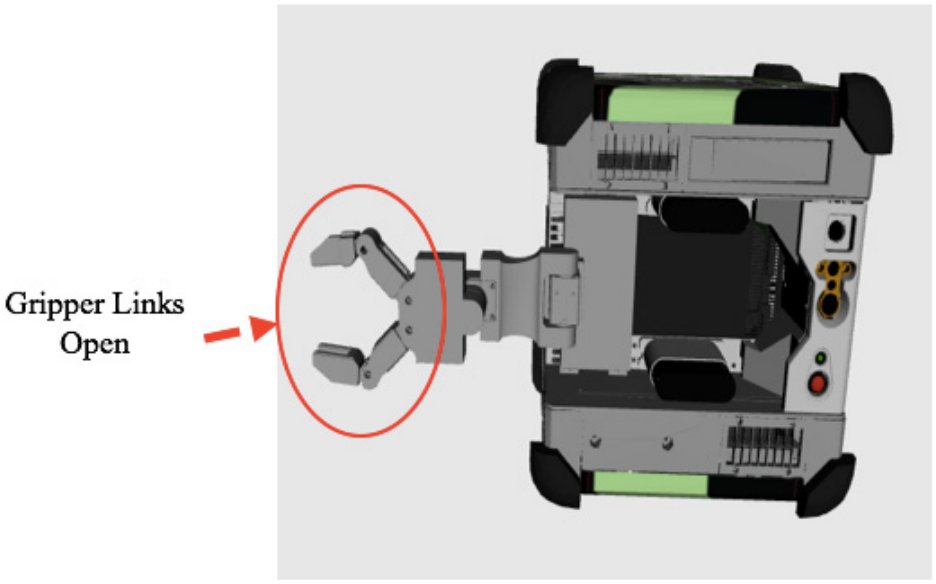

Figure 15. Gripper Links in the Open Position. View from the Top of Astrobee.

Astrobee's manipulator pan range and tilt are as identified in Figure 16 and Figure 17, respectively.

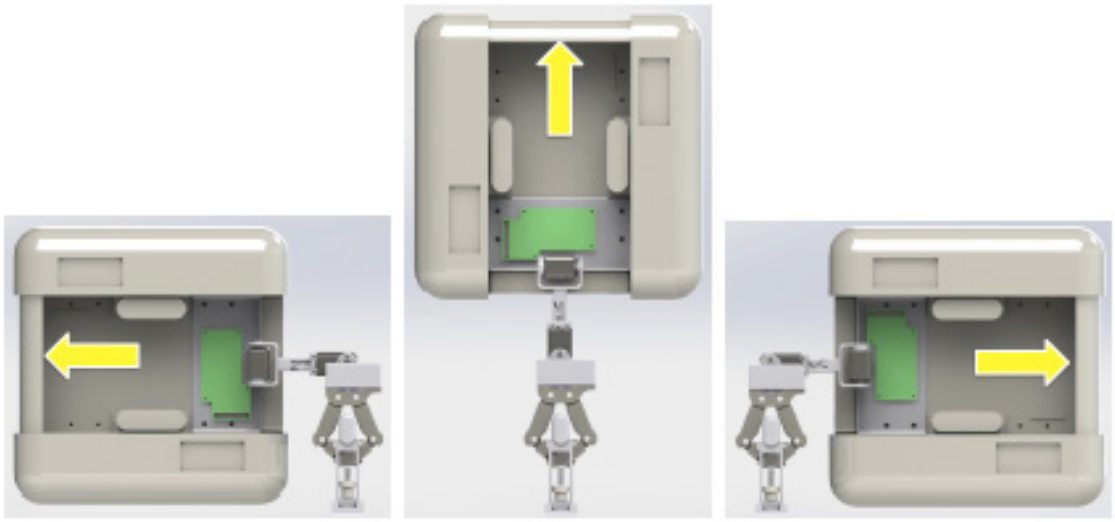

Figure 16. Pan range of -90° to 90° for Astrobee. Source: Park et al. (2017).

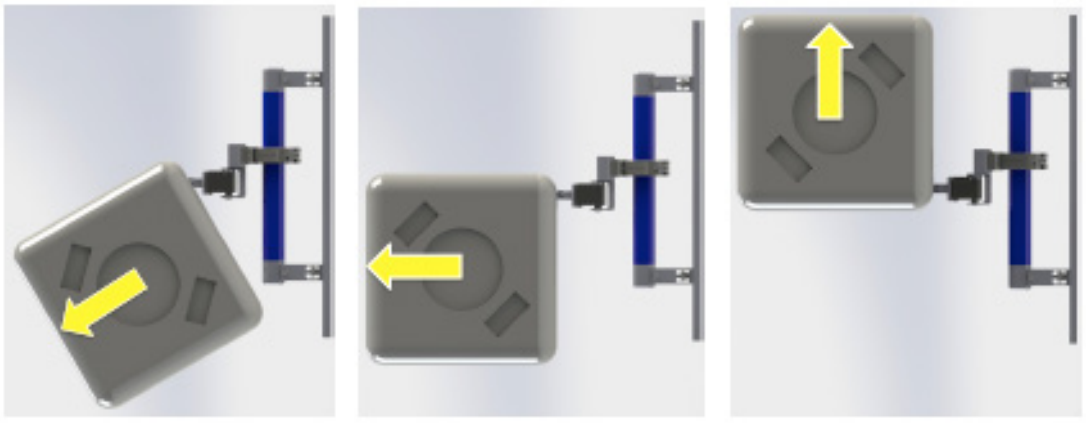

Figure 17. Tilt range of -30° to 90° for Astrobee. Source Park et al. (2017).

The mass and principal moments of inertia properties of the system are given in Table 3.

Table 3. Astrobee Manipulator: Mass and Inertia Parameters. Source: NASA (2018).

Link	**Mass [kg]**	**Principal Moments of Inertia [kg m^2]**		
		I_{xx}	**I_{yy}**	**I_{zz}**
Base	7	0.1083	0.1083	0.1083
Arm Proximal	0.1623	0.02705	0.02705	0.02705
Arm Distal	0.1033	0.002705	0.002705	0.002705
Gripper Left Proximal	0.04	0.002705	0.002705	0.002705
Gripper Left Distal	0.0116	0.002705	0.002705	0.002705
Gripper Right Proximal	0.04	0.002705	0.002705	0.002705
Gripper Right Distal	0.02285	0.002705	0.002705	0.002705

The linear velocity envelope of what Astrobee's joints and links are capable of achieving are displayed in Figures Figure 18 and Figure 19. The results indicate that Astrobee can conduct a hopping maneuver in any direction. The results also indicate that Astrobee can push itself off the handrail and perch itself back on the same handrail. More importantly, the data shows that the max velocity of the hopping maneuver does not exceed

the max velocity of the joints or the max velocity (~2.1 m/s) for free-flying robots in the ISS (Smith et al. 2016).

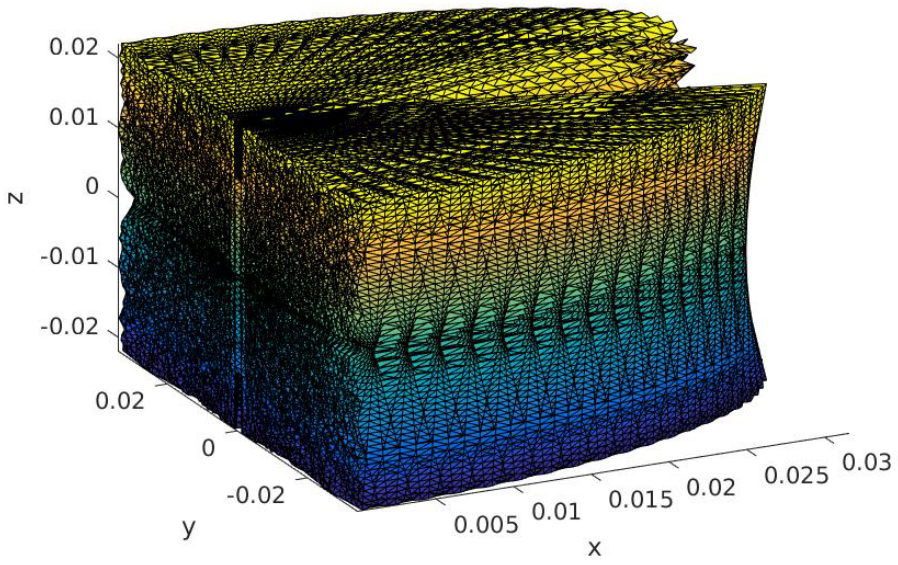

Figure 18. Linear Velocity Envelope [m/s].

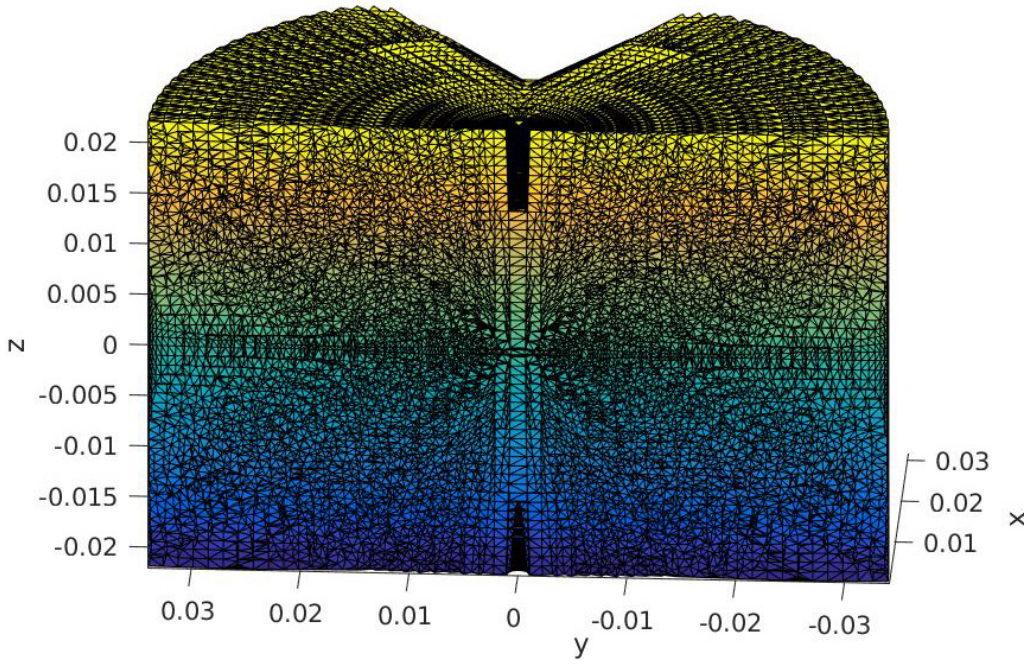

Figure 19. Linear Velocity Envelope [m/s].

B. A PLANAR HOP WITH ASTROBEE

A planar hopping maneuver reduces the dynamics of the problem to a 2D planar motion, with the initial position of Astrobee's Arm Proximal Joint extended from the handrail at a determined height. The spacecraft completes the maneuver rotating about a single axis. The contact dynamics for the release are idealized and the grippers are opened and closed at the same rate so as to have no collisions with the gripper and the handrail. When the grippers are commanded open, the grippers release with no additional friction or delay. Further ground-based experiments must be conducted to verify if the real-world dynamics are equal to the idealized conditions for the simulation experiment with Astrobee.

C. SIMULATION EXPERIMENT WITH ASTROBEE

Due to software limitations, the application velocity to joints was infeasible. As such, to accomplish this planar hopping experiment, the only control variable is the configuration of the manipulator at the point of release. The range of possible ranges of the manipulator at release for a hard-landing hopping maneuver are found in Table 4. The height and range values in Table 4 can be correlated to the schematic of the hard-landing displayed in Figure 20.

Table 4. Hard-Landing Correlation between Height and Range Via the Release Configuration of the Arm Proximal Joint.

Height [m]	Arm Proximal [rad]	Range [m]
0.282	-2.094	1.025
0.368	-2.010	0.998
0.452	-1.925	0.965
0.532	-1.841	0.924
0.609	-1.756	0.877
0.682	-1.671	0.823
0.749	-1.587	0.763
0.812	-1.502	0.697
0.868	-1.417	0.627
0.919	-1.333	0.551
0.962	-1.248	0.472
0.999	-1.164	0.389
1.029	-1.079	0.303
1.051	-0.994	0.215
1.065	-0.910	0.126
1.072	-0.825	0.035

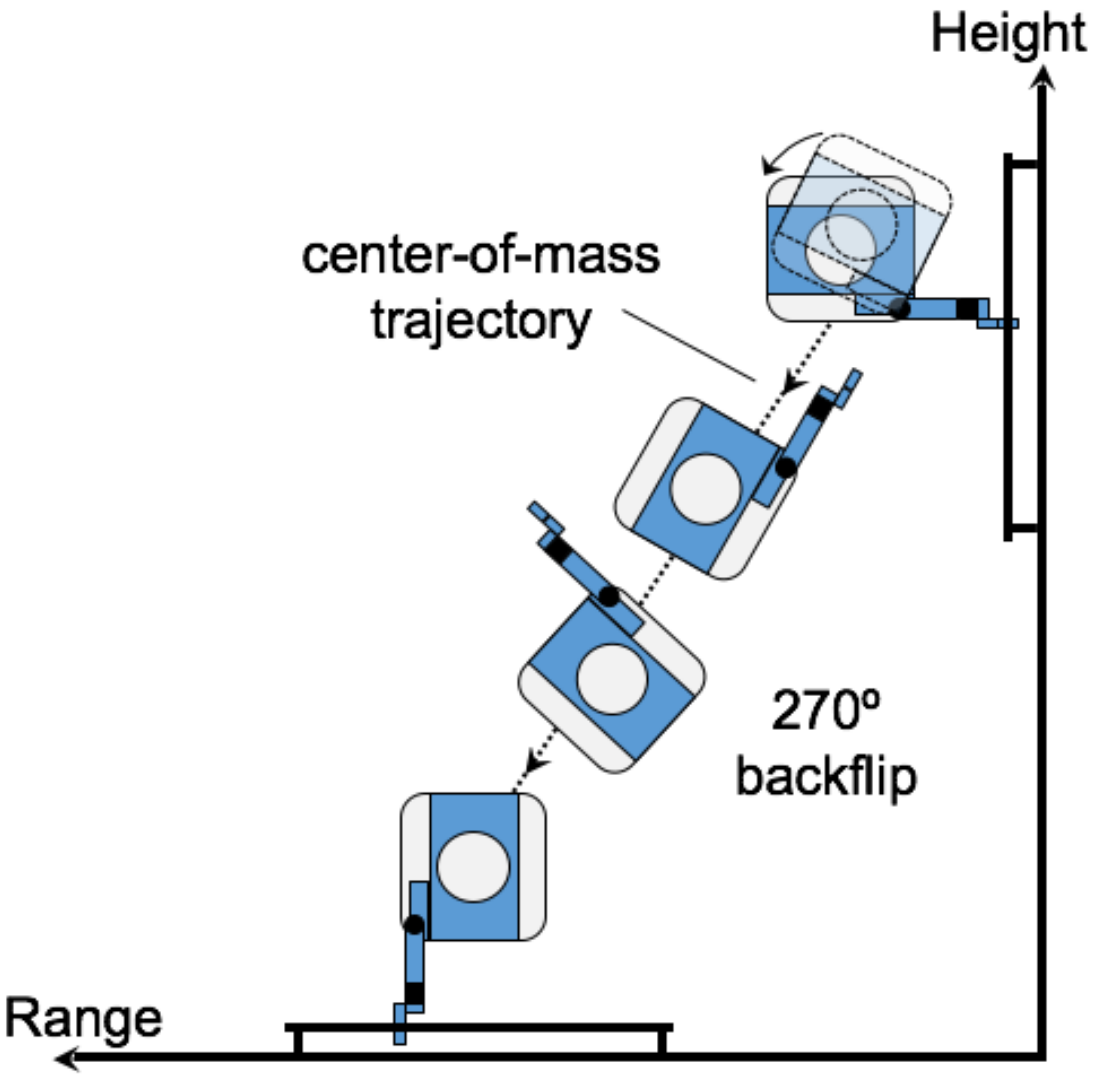

Figure 20. Schematic of Astrobee Completing a Hard-Landing.

Table 5 provides the range the manipulator configurations for the Arm Proximal at time at of release for a soft-landing. The height and range values in Table 5 are correlated to Figure 21. A soft-landing includes actuation of the manipulator during the free-fly coast phase opposite the rotation of the base to negate the angular momentum of the system prior to landing.

Table 5. Soft-Landing Correlation between Height and Range Via the Release Configuration of the Arm Proximal Joint.

Height [m]	Arm Proximal [rad]	Range [m]
0.3307	-2.094	0.7553
0.4388	-2.022	0.7384
0.4301	-1.950	0.7177
0.4911	-1.950	0.7177
0.5441	-1.878	0.6933
0.5909	-1.806	0.6653
0.6544	-1.733	0.6339
0.7038	-1.733	0.6339
0.7421	-1.667	0.5992

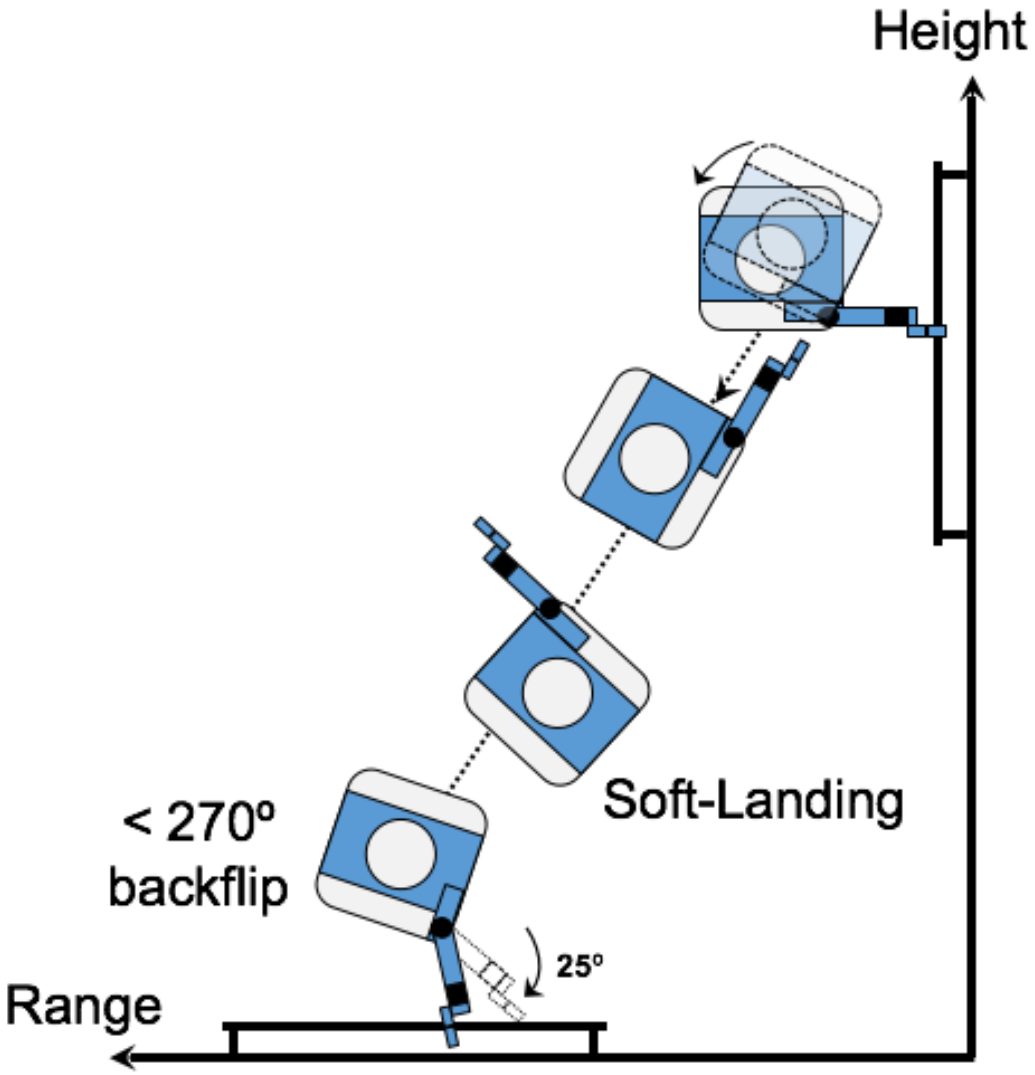

Figure 21. Schematic of Astrobee Completing a Soft-Landing.

D. INITIALIZATION MODE

When the hopping maneuver is initiated, the initial position of Astrobee is measured and compared with Table 4 to determine the corresponding Arm Proximal joint configuration associated with the height of Astrobee. The initial position of Astrobee perched on handrail is pictured in Figure 22.

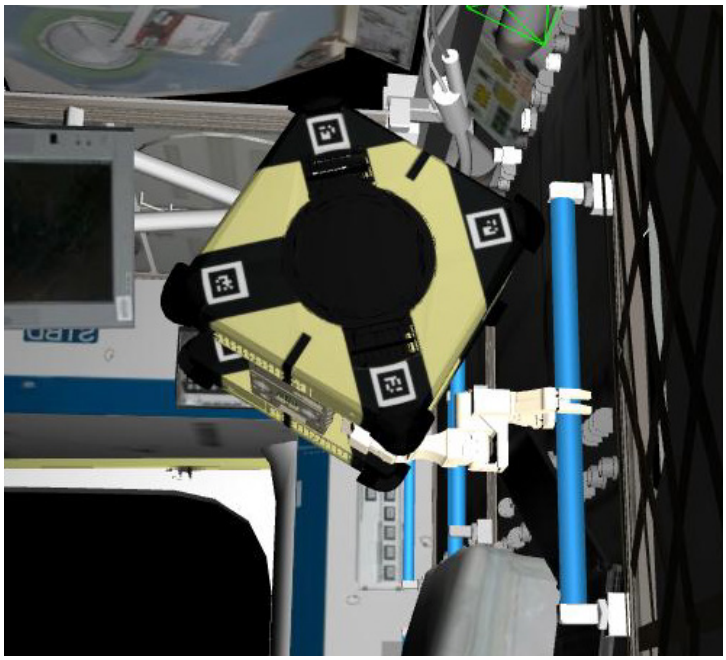

Figure 22. Astrobee Perched on ISS Handrail in Simulated ISS Environment.

Table 4 and Table 5 provide the release configuration, $\boldsymbol{q_m}$ at the exact moment of release and the associated height and range of the hopping maneuver.

1. Inputs

The inputs to the initialization mode controller are:

(a) $\boldsymbol{q}_m$: The joint positions of the manipulator.

(b) $\dot{\boldsymbol{q}}_m$: The velocities of the manipulator joints.

Prior to initialization mode, Astrobee is positioned in a random location and configuration. The onboard sensors of Astrobee determine the location of the robot and hopping maneuver software determines the inputs for the initialization mode calculated in Table 4 and Table 5 for the respective maneuver. The inputs are then fed into the initialization controller. The two inputs correspond to one revolution of Astrobee for a successful hopping maneuver.

2. Outputs

The outputs to the initialization mode controller are:

(a) $\boldsymbol{\tau}_m$: Torque applied to manipulator.

(b) $\boldsymbol{\tau}_0$: Torque applied to base-spacecraft.

(c) $\boldsymbol{F}_0$: Force on the base-spacecraft.

(d) Completion flag: Indication that the maneuver has been completed.

Output from the initialization controller command Astrobee to the push configuration with the grippers rigidly attached to the handrail. Completion flag signals that the controller has completed all tasks and is ready to enter the next mode.

3. Completion Criteria

The initialization mode controller measures the initial position and orientation of Astrobee, with a closed gripper, rigidly attached to the handrail, and then imparts a proportional feedback controller to command the joints of Astrobee to the required configuration to complete the hopping maneuver. The completion criteria are:

(a) $\boldsymbol{q_{m\_ref}} - \boldsymbol{q_m} = \boldsymbol{q_{m\_thres}}$ where $\boldsymbol{q_{m\_thres}} = 0.1$ deg

(b) $\dot{\boldsymbol{q}}_{\boldsymbol{m\_ref}} - \dot{\boldsymbol{q}}_{\boldsymbol{m}} = \dot{\boldsymbol{q}}_{\boldsymbol{m\_thres}}$ where $\dot{\boldsymbol{q}}_{\boldsymbol{m\_thres}} = 0.05$ deg/s

When both criteria are met, the initiation mode is complete and enables the push mode.

E. PUSH MODE

The push initiates on the receipt of the completion flag from the initialization mode.

1. Inputs

The inputs to the push mode controller are:

(a) $\boldsymbol{q}_m$: The joint positions of the manipulator.

(b) $\dot{\boldsymbol{q}}_m$: The velocities of the manipulator joints.

2. Outputs

The outputs to the push mode controller are:

(a) $\boldsymbol{\tau}_m$: Torque applied to manipulator.

(b) $\boldsymbol{\tau}_0$: Torque applied to base-spacecraft.

(c) $\boldsymbol{F}_0$: Force on the base-spacecraft.

(d) Completion flag: Indication that the maneuver has been completed.

Output from the push controller indicates Astrobee ready to release from the handrail at the determined manipulator configuration. Completion flag signals that the controller has completed all tasks and is ready to enter the next mode.

3. Completion Criteria

The push actuates the joints of Astrobee and imparts a proportional feedback controller to command Astrobee to the proper release position $\boldsymbol{q}_{\boldsymbol{m}_1^{release}}$ where $\boldsymbol{q}_1$ was calculated in the initiation mode based off of initial position of Astrobee. The completion criteria are:

(a) $\left(\boldsymbol{q}_{\boldsymbol{m}_1} - \boldsymbol{q}_{\boldsymbol{m}_1^{release}}\right) * \boldsymbol{sign}(\boldsymbol{\tau}) > \boldsymbol{0}$

(b) $\boldsymbol{q}_{\boldsymbol{m}_1^{release}} = \boldsymbol{q}_1$

When both criteria are met, the push mode is complete and the free-flying coast mode is enabled.

F. FREE-FLYING PASSIVE COAST MODE

1. Inputs

The inputs to the free-flying passive coast mode controller are:

(a) $\boldsymbol{q}_m$: The joint positions of the manipulator.

(b) $\dot{\boldsymbol{q}}_m$: The velocities of the manipulator joints.

(c) $\boldsymbol{r}_0$: Position of base-spacecraft

(d) $\boldsymbol{DCM}_{BN}$: Direction Cosine Matrix – Body frame to inertia frame

2. Outputs

The outputs to the free-flying passive coast mode controller are:

(a) $\boldsymbol{\tau}_m$: Torque applied to manipulator.

(b) $\boldsymbol{\tau}_0$: Torque applied to base-spacecraft.

(c) $\boldsymbol{F}_0$: Force on the base-spacecraft.

(d) Time: Log time.

(e) Completion flag: Indication that the maneuver has been completed.

Output from the free-fly coast controller indicates Astrobee has released from the handrail and is in free-flying passive coast mode with the manipulator fixed in the release configuration. Completion flag signals that the controller has completed all tasks and is ready to enter the next mode.

3. Completion Criteria

Astrobee's manipulator is held fixed to the release position $\boldsymbol{q}_{\boldsymbol{m}_1^{release}}$. The completion criteria is:

(a) $dot(\boldsymbol{r}_{COM}\boldsymbol{q}_0) - \boldsymbol{z}_{thres} > \boldsymbol{0}$ where $\boldsymbol{z}_{thres} = 0$.

The $\boldsymbol{z}_{thres}$ is set to zero for the hard-landing maneuver as the gripper will not move prior to grasping the handrail.

When the completion criteria is met, the free-flying coast passive mode is complete and the free-flying active coast mode is enabled.

G. FREE-FLYING COAST ACTIVE MODE

1. Inputs

The inputs to the free-flying active coast mode controller are:

(a) $\boldsymbol{q}_m$: The joint positions of the manipulator.

(b) $\dot{\boldsymbol{q}}_m$: The velocities of the manipulator joints.

(c) $\boldsymbol{r}_0$: Position of the base-spacecraft.

(d) Time: Logged time.

(e) $\boldsymbol{DCM}_{BN}$: Direction Cosine Matric: Body frame to inertial frame.

2. Outputs

The outputs to the free-fly active coast mode controller are:

(a) $\boldsymbol{\tau}_m$: Torque applied to manipulator.

(b) $\boldsymbol{\tau}_0 = 0$

(c) $\boldsymbol{F}_0 = 0$

(d) Time: Log time.

(e) Completion flag: Indication that the maneuver has been completed.

Outputs from the free-flying active coast controller indicate Astrobee is in free-flying active coast mode with the manipulator actively moving to negate the angular velocity. Completion flag signals that the controller has completed all tasks and is ready to enter the next mode.

3. Completion Criteria

Astrobee's manipulator is no longer held fixed to the release position $\boldsymbol{q}_{\boldsymbol{m}_1^{release}}$ but is moving to counter the rotation of Astrobee to enable a soft-landing. If a hard-landing has been programed, this mode will not be entered. The completion criteria is:

(a) $dot(\boldsymbol{r}_{COM}\boldsymbol{q}_0) - \boldsymbol{z}_{thres} > \boldsymbol{0}$ where $\boldsymbol{z}_{thres} = 0$.

The $\boldsymbol{z}_{thres}$ is set to zero for the soft-landing maneuver. The initial position of the base of Astrobee was increased to allow time for the manipulator to ramp up to the needed velocity. The manipulator must be opposite and equal to the rotation of the base to negate the angular rotation of the spacecraft. The moment the velocity of the manipulator equals the velocity of the rotation of the spacecraft, the gripper will grasp the handrail.

When the completion criteria is met, the free-flying coast active mode is complete and the landing mode is enabled.

H. SELF-STABILIZER MODE

The stabilizer controller is the only controller that actively uses propellant. The purpose of this controller is to act as a safety-net in the event the spacecraft needs to cancel hopping maneuver.

1. Inputs

The inputs to the stabilization mode controller are:

(a) $\boldsymbol{q}_m$: The joint positions of the manipulator.

(b) $\dot{\boldsymbol{q}}_m$: The velocities of the manipulator joints.

(c) $\boldsymbol{r}_0$: Position of the base-spacecraft.

(d) $\dot{\boldsymbol{r}}_0$: Velocity of the base-spacecraft.

(e) $\boldsymbol{q}_{BN}$: Quaternion from base frame to inertial frame.

(f) $\boldsymbol{\omega}_{BN}$: Angular momenta from base frame to inertial frame.

(g) $\boldsymbol{DCM}_{BN}$: Direction Cosine Matrix: Base frame to inertial frame.

2. Outputs

The outputs to the stabilization mode controller are:

(a) $\boldsymbol{\tau}_m$: Torque applied to manipulator.

(b) $\boldsymbol{\tau}_0$: Torque applied to base-spacecraft.

(c) $\boldsymbol{F}_0$: Force on the base-spacecraft.

(d) Completion flag: Indication that the maneuver has been completed.

Outputs from the stabilization controller indicates Astrobee has released from the handrail and is stable in a centralized location safe from colliding with the walls of the ISS.

Completion flag signals that the controller has completed all tasks and Astrobee remains in a hover position.

3. Completion Criteria

Astrobee's manipulator is held fixed to the release position $\boldsymbol{q}_{m_1^{release}}$. The completion criteria are:

(a) time $> 5\ seconds$

(b) Astrobee positioned at the (0,0,0)

When the completion criteria are met, the stabilization mode is complete and the maneuver is disabled.

I. LANDING MODE

The passive actuation of the proximal joint is defined in the final landing phase as a hard-landing if the robotic manipulator remains stationary during the coast phase. The manipulator remains stationary in order to keep the release configuration equal to the catch configuration. The spacecraft will complete a 270 degree rotation from handrail to handrail. The proximal joint deflection is the only control variable and the starting height with the joint deflection determine the landing location.

To achieve a softer-landing, approximately the last five seconds of the hopping maneuver, immediately prior to perching, the hopping spacecraft will actuate the proximal joint to eliminate the relative angular velocity. The absence of angular velocity by definition will achieve a relative velocity of zero between the hopping vehicle and the stationary handrail, which creates the desired effect of a "soft-landing." An ideal relative velocity of zero is not possible with Astrobee due to the DOF of the manipulator. The angular velocity can be eliminated but not the linear velocity. Prior to the hopping maneuver, the required joint deflection for the ramp up of the soft-landing is a fixed parameter. The actuation of the proximal joint changes the spacecraft's rotation.

1. Inputs

The inputs to the Landing mode controller are:

(a) $\boldsymbol{q}_m$: The joint positions of the manipulator.

(b) $\dot{\boldsymbol{q}}_m$: The accelerations of the manipulator joints.

2. Outputs

The outputs to the stabilization mode controller are:

(a) $\boldsymbol{\tau}_m$: Torque applied to manipulator.

(b) $\boldsymbol{\tau}_0$: Torque applied to base-spacecraft.

(c) $\boldsymbol{F}_0$: Force on the base-spacecraft.

(d) Completion flag: Indication that the maneuver has been completed.

Outputs from the landing controller indicate Astrobee has caught the handrail. Completion flag signals that the controller has completed all tasks and the hopping maneuver is complete.

3. Completion Criteria

Astrobee's manipulator is in the catch position and Astrobee is rigidly grasping the ISS handrail. The completion criteria are:

(a) $\dot{\boldsymbol{q}}_m = 0$: The accelerations of the manipulator joints.

When the completion criteria are met, the hopping maneuver is complete.

J. CONCLUSION

Planar hopping maneuver is possible with NASA - Ames Research Center's Free-flyer, Astrobee. The release configuration of the manipulator is the only control variable for a planar hopping maneuver with Astrobee. As such, height and range are associated with the release configuration. Due to the DOF of Astrobee's manipulator, achieving a soft-landing is only applicable in negating the angular velocity. Future work includes, targeting a specific range by moving the manipulator during free-flying coast phase and creating a more versatile manipulator with additional DOF to negate the linear velocity of Astrobee to truly achieve a relative velocity of zero in the soft-landing.

THIS PAGE INTENTIONALLY LEFT BLANK

IV. SIMULATION RESULTS

Results from numerical simulation experiments are presented in this chapter. Two simulation experiments were conducted to verify the hopping maneuver concept. The first of the simulation experiments is the demonstration of the hard-landing with the passive proximal joint deflection. The second simulation experiment is the implementation of the soft-landing proximal-joint actuation. All experiment results verify the hopping maneuver concept and provide data to be compared with ground based tests. Purpose of simulation and ground based testing is to validate the hopping maneuver concept and the likelihood of a successful hopping maneuvers in zero-gravity environment.

A. HARD-LANDING HOPPING SIMULATION

Simulation begins with Astrobee perched on the handrail. Moments before the time of release, the proximal joint is actuated to create the push mode. The simulation imposes a constant velocity on the joint until the proximal joint matches the defined release configuration. The deflection then stops, the joint velocity is now zero, and Astrobee enters into free-fly coast mode. During this phase, the proximal joint is held fixed. The landing mode is the mode in which Astrobee catches the handrail at the final location inside the simulated ISS environment. Figure 23 illustrates the hopping maneuver and defines the terms range and height with respect to the experiment set up. Figure 24 displays the results of the simulated hopping maneuvers, displaying the height and range of 14 hopping maneuvers all of which are within the range of values described in Table 4. Astrobee begins at a given height located on the right hand side of the graph and ends the maneuver at a determined range (Table 4) on the left hand side of the graph. The figure has the height defined on the right-hand axis label to visually mirror the experiment seen in the schematic of Figure 23.

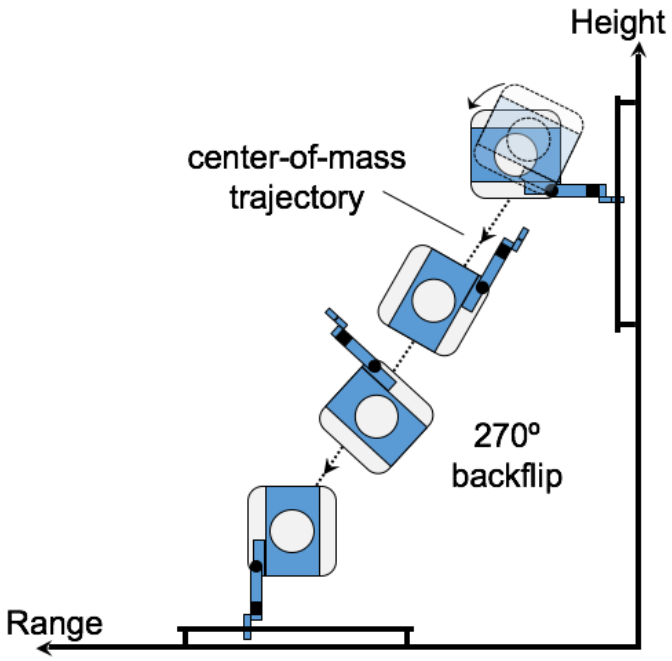

Figure 23. Schematic of Astrobee Completing a Hard-Landing.

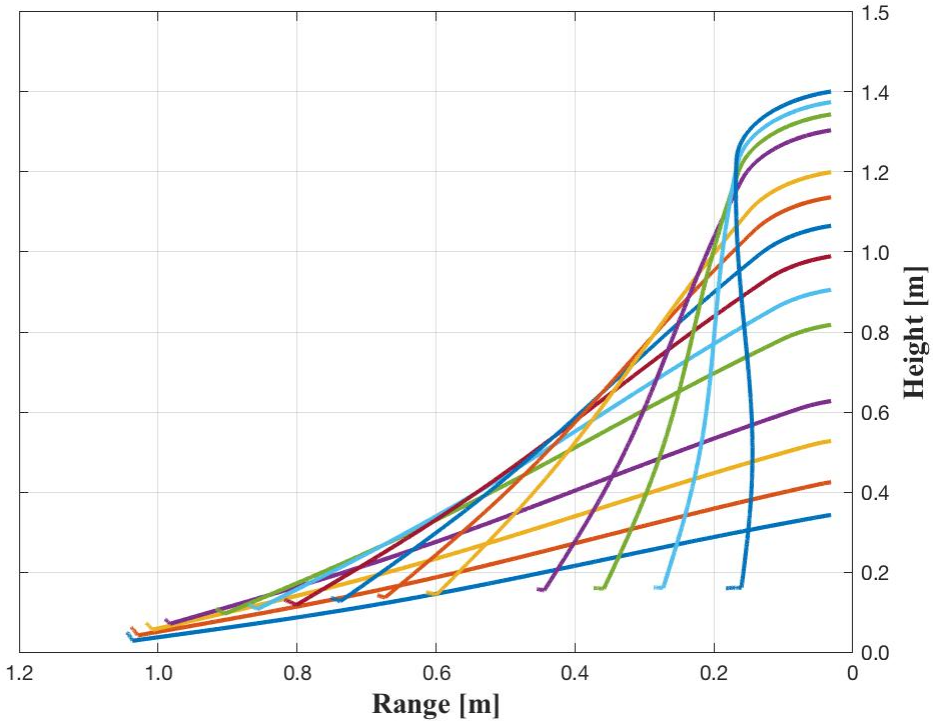

Figure 24. Location of Base during Hard-Landing Hopping Maneuver.

The proximal joint deflection over the span of the hopping maneuvers are displayed in Figure 25. The proximal joint is actuated for the push phase and then held fixed for the duration of the hopping maneuver indicated by the straight line in Figure 25. During the catch phase, the proximal joint is again actuated to grasp the handrail and complete the hopping maneuver.

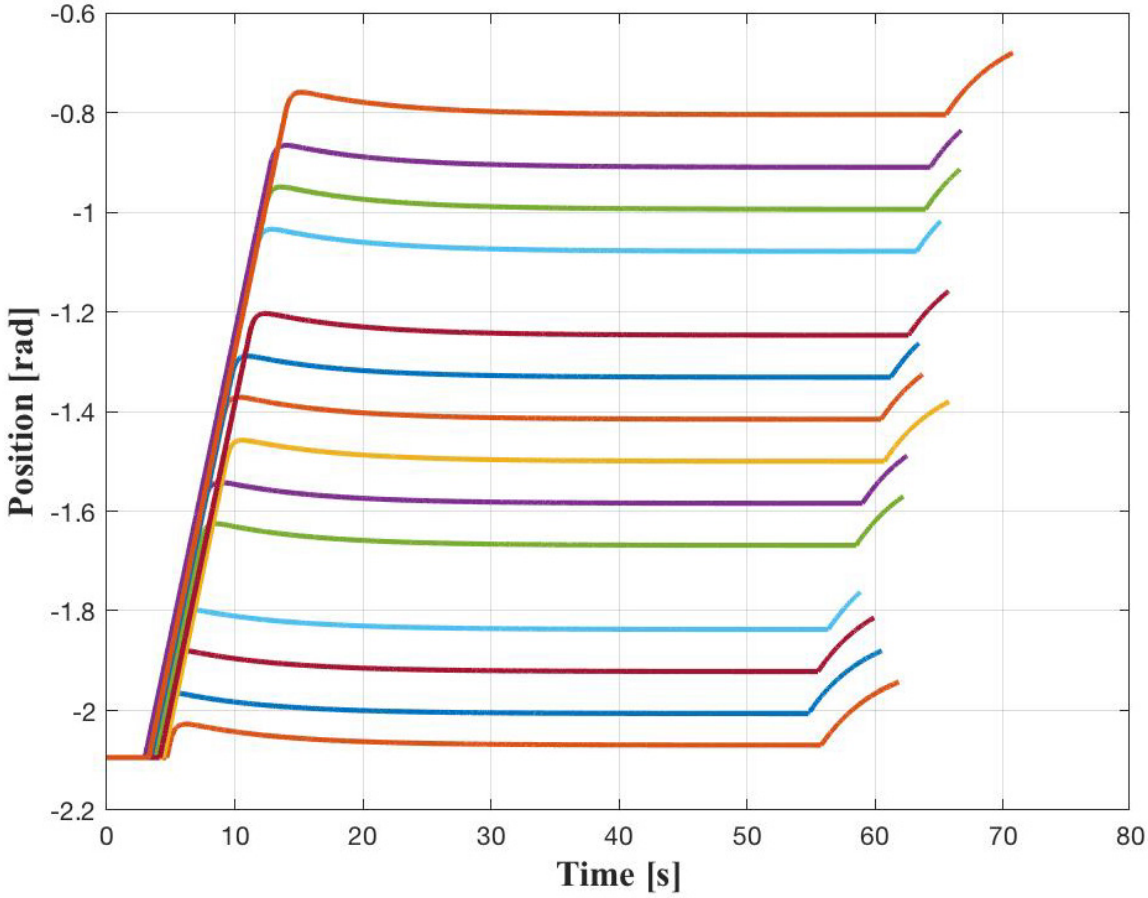

Figure 25. Hard-Landing Proximal Joint Position

The forces experienced during the maneuver are of interest and are displayed in Figure 26. The results indicate that approximately 2 Newton of force are experienced during the push. Ground based experiments will test the dynamics with real-world environments. The ground based experiments will need to be less than 2 Newton for these simulated experiments to verify the hopping maneuver concept.

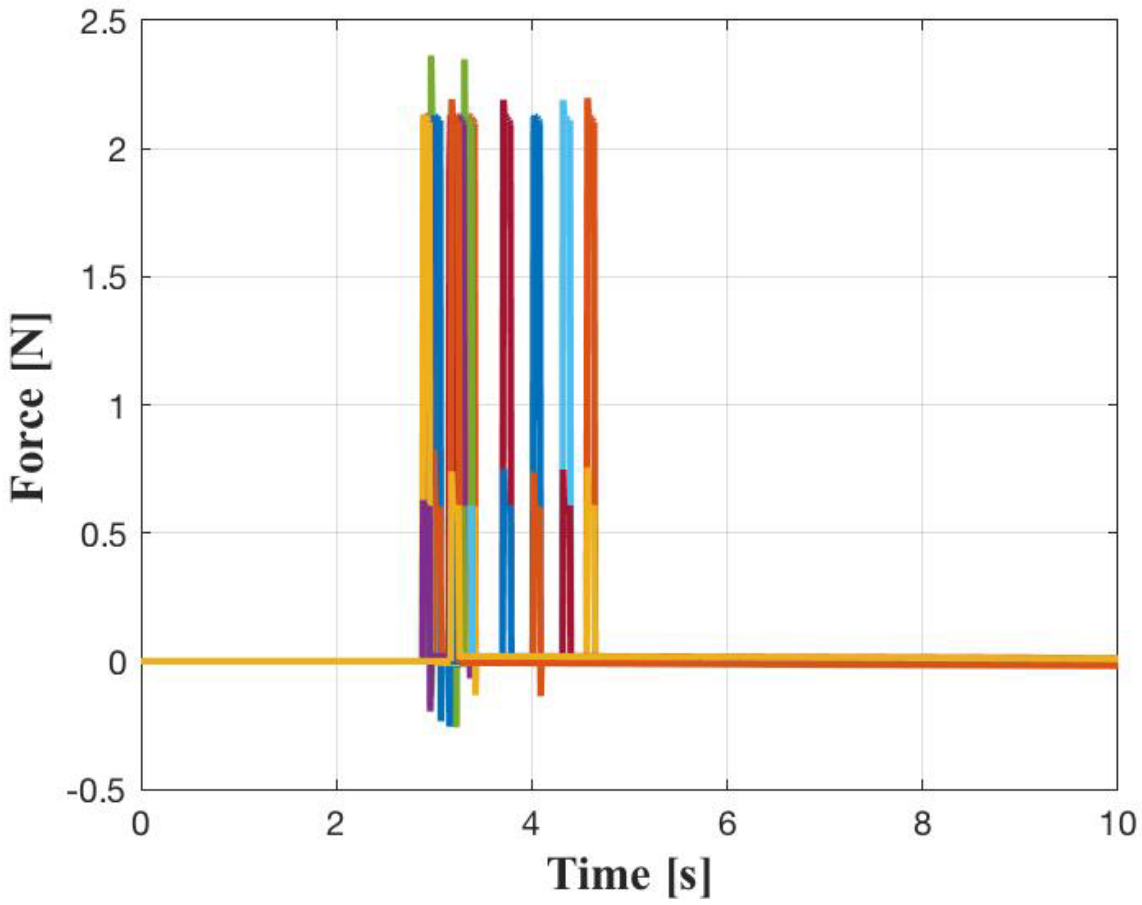

Figure 26. Forces During Push Phase of Hard-Landing Hopping Maneuver.

B. SOFT-LANDING HOPPING SIMULATION

Simulation begins with Astrobee perched on the handrail. Moments before the time of release, the proximal joint is actuated to make up the push mode. Once the proximal joint reaches the release configuration, the deflection stops as Astrobee enters into free-fly coast mode. During the majority of this phase, the proximal joint is held fixed until the simulation enters active joint landing in which the joint is no longer held fixed and moves to counter the angular velocity. The landing mode is the mode in which Astrobee catches the handrail at the final location inside the simulated ISS environment. Figure 27 illustrates the soft-landing hopping maneuver and defines the terms range and height with respect to the experiment set up. Figure 28 displays the results of the simulated hopping maneuvers, displaying the height and range of 10 hopping maneuvers all of which are within the range

of values described in Table 5 . Astrobee begins at a given height located on the right hand side of the graph and ends the maneuver at a determined range (Table 5) on the left hand side of the graph. The figure has the height defined on the right-hand axis label to visually mirror the experiment seen in the schematic of Figure 27.

Changes to the hard-landing are as follows. The software is not changed but rather the hard-landing command never enters active joint phase of the free-flying coast whereas soft-land not only completes the free-flying coast passive joint but then enters the active joint phase.

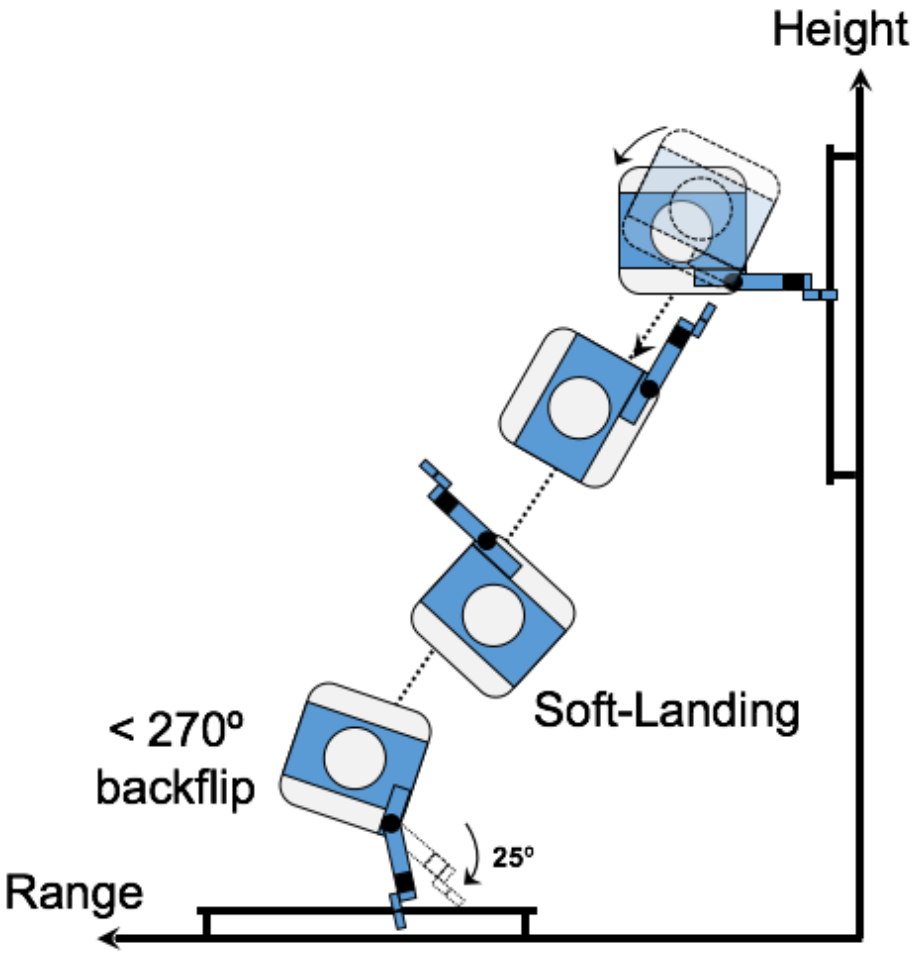

Figure 27. Schematic of Astrobee Completing a Soft-Landing.

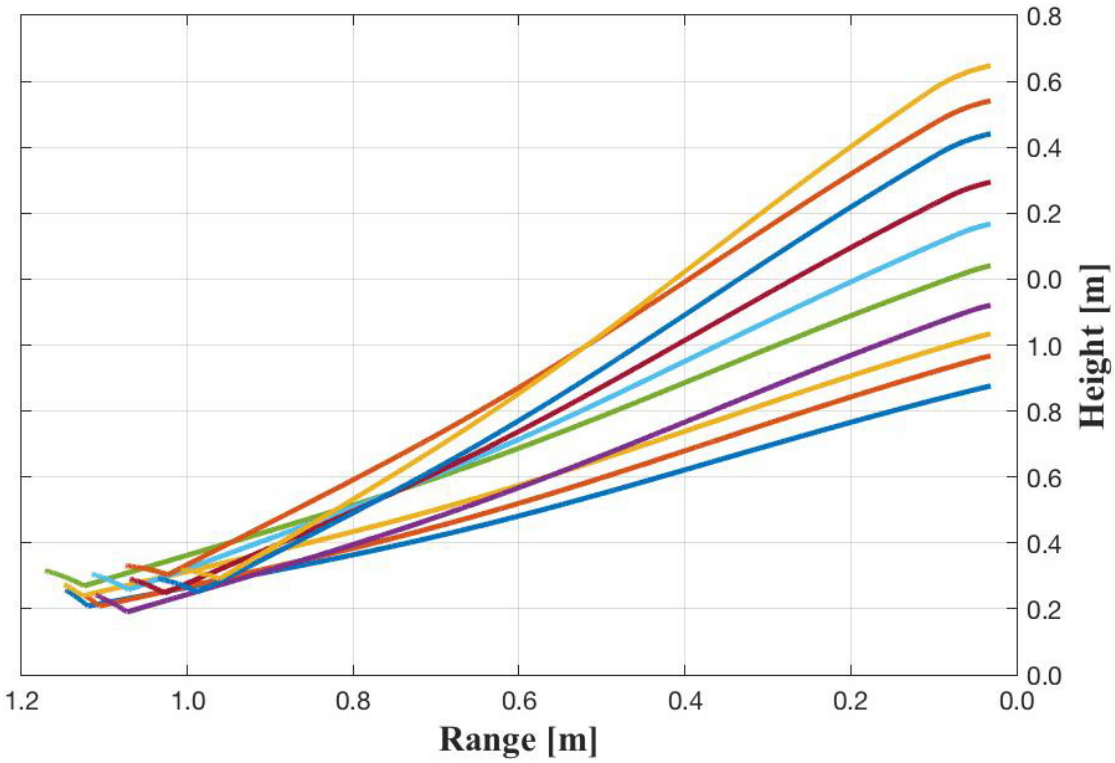

Figure 28. Location of Base during Soft-Landing Hopping Maneuver.

The proximal joint deflection over the span of a hopping maneuver are displayed in Figure 29. The proximal joint is actuated for the push and actuated again prior to the catch indicated by the rounded curve near the end of the maneuver. During the catch phase, the grippers grasp the handrail and complete the hopping maneuver.

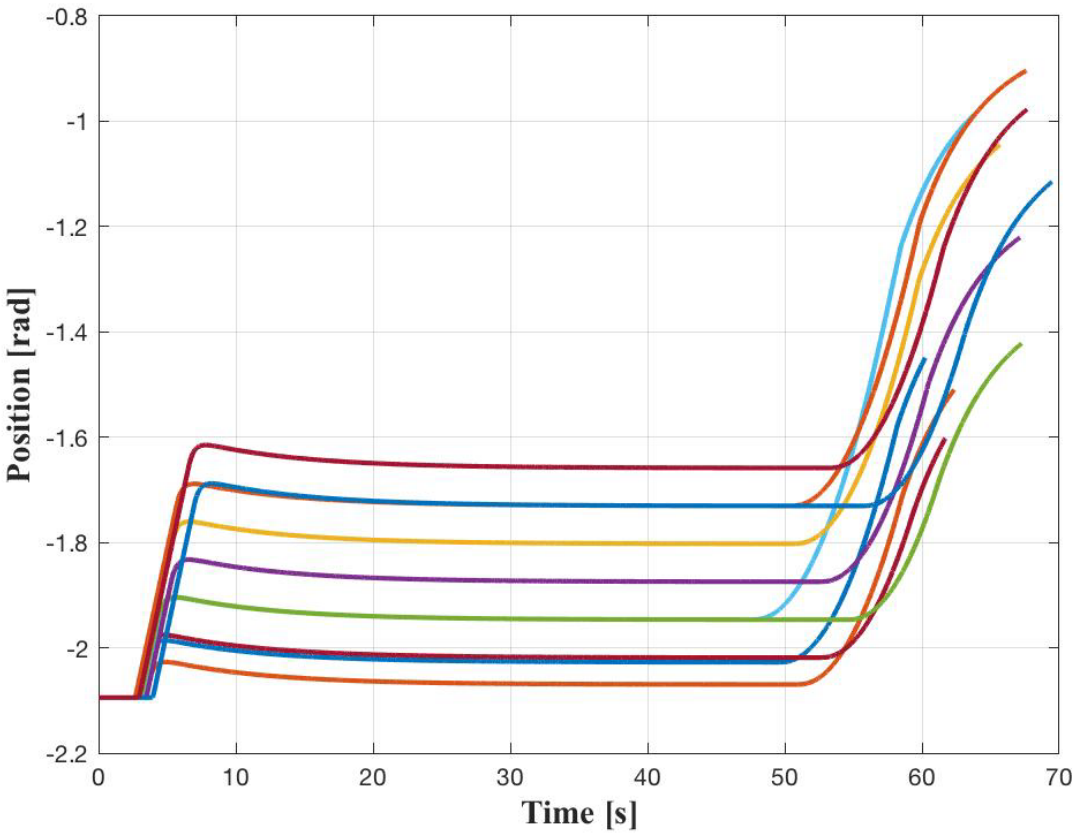

Figure 29. Soft-Landing Proximal Joint Position

The forces experienced during the maneuver are of interest and are displayed in Figure 30. The results indicate that approximately 2 Newton of force are experienced during the push. Ground based experiments will test the dynamics with real-world environments. The ground based experiments will need to be less than 2 Newton for these simulated experiments to verify the hopping maneuver concept.

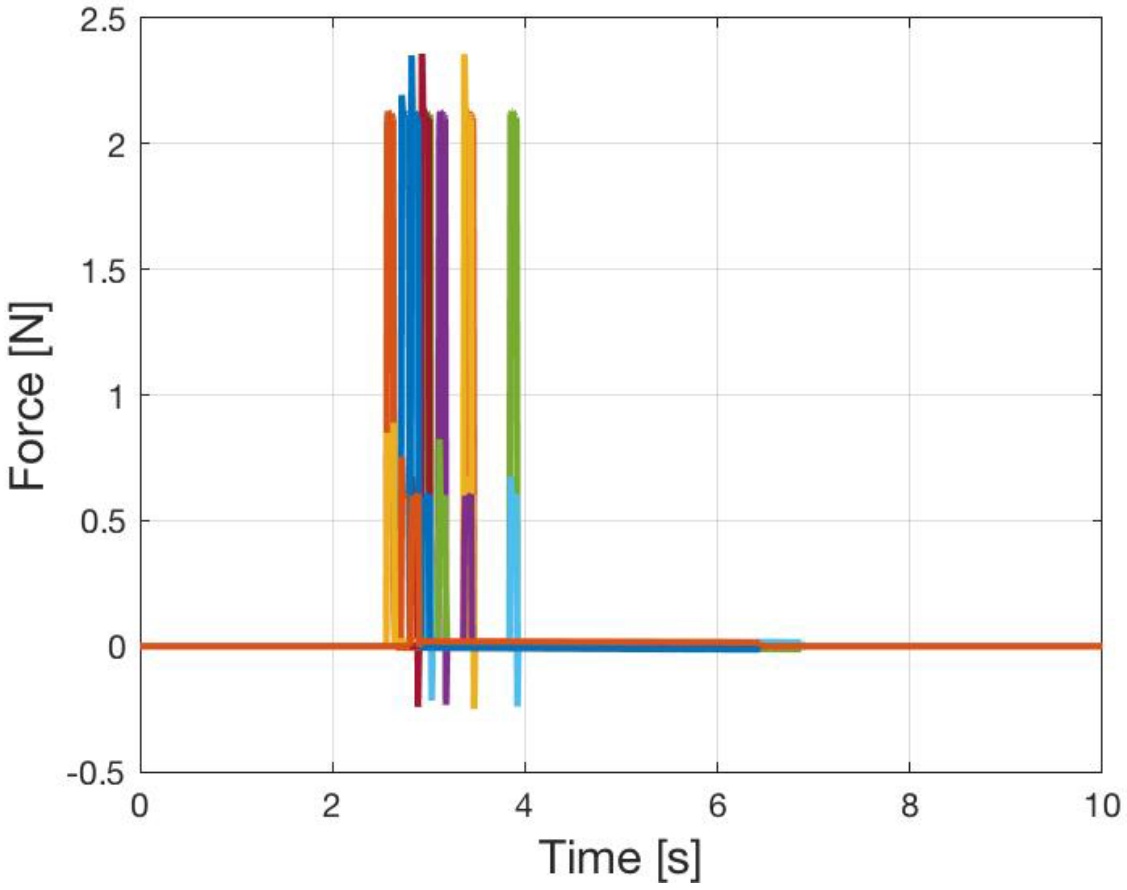

Figure 30. Forces during the Push Phase of Soft-Landing Hopping Maneuver.

C. CONCLUSION

Planar hopping maneuver is possible with NASA – Ames Research Center's Free-flyer, Astrobee. The release configuration of the manipulator is the only control variable for a planar hopping maneuver with Astrobee. As such, the height and range are associated with the release configuration. Due to the DOF of Astrobee's manipulator, achieving a soft-landing is only applicable in negating the angular velocity. Future work includes, targeting a specific range by moving the manipulator during free-flying coast phase and creating a more versatile manipulator with additional DOF to negate the linear velocity of Astrobee to truly achieve a relative velocity of zero in the soft-landing.

V. PLANNED ISS EXPERIMENT

The ISS provides a safe environment to conduct zero-gravity experiments for hopping maneuvers. Research facilities onboard the ISS support a risk free platform to conduct microgravity experiments. The dynamic environment of the ISS are ideal for testing guidance and control algorithms for maneuverability of spacecraft in space. Astrobee provides the robotic vehicle necessary to demonstrate advanced control algorithm and will be the platform of choice for this thesis. Through guest scientist research, this thesis experiment is capable of implementation onboard the ISS. Bi-weekly meetings with the NASA - Ames Research team and quarterly updates to the SPHERES/Astrobee working group provided the ground work necessary to make this thesis experiment possible with fastest integration to NASA's flight software. Accessibility to the ISS research facility where Astrobee will conduct the experiments is limited to software updates only to the robotic vehicle via NASA - Ames Research Center control center.

As a Department of Defense entity, Space Experiments Review Board (SERB) approval is required to get approval to run an experiment onboard the ISS and to be added to a mission manifest. The objective for conducting a hopping maneuver onboard the ISS is to conduct on-orbit demonstration of the hopping mobility approach. The approved mission manifest and the concept of operations for the experiment setup is discussed in detail in this chapter. The impact of this on-orbit demonstration is to advance orbital robotics technology with application to include on-orbit servicing and assembly of large apertures in space.

A. CONCEPT OF OPERATION

Mission manifest includes five on-orbit experiment sessions. The scheduled sessions are designed in such a way to increase in complexity allowing time to implement lessons learned between experiment sessions. Table 6 identifies the goals for each session. Sessions are scheduled for three-hour time slots. The first three experiments require reserved astronaut time to provide a safety net for the robot in the case of unexpected telemetry. One of the three Astrobee that is not involved in the maneuver will also act as a

third party observer along side the astronauts but unlike the astronauts the robot will not be able to reposition the maneuvering Astrobee or reset the robot as needed for the duration of the experiment.

Table 6. Five Approved Experiment Sessions Onboard ISS.

S1	Explore push maneuvers. Termination during coast.
S2	Push aiming at target handrail. Termination during coast.
S3	Hopping with propulsive stabilization prior to handrail-perching.
S4	Complete hop maneuver. Push, free-fly, and soft-land.
S5	Margin.

B. QUALITY OF THE EXPERIMENT

On-orbit demonstration of the hopping maneuver will be the first on-orbit demonstration of a propellantless hopping maneuver. Successful laboratory testing and numerical simulations suggest high likelihood of success. Advances orbital robotic mobility, complementing to other Department of Defense (DoD) research programs.

C. PLAN OF IMPLEMENTATION

This experiment is low-risk and low-cost due to the integration with Astrobee strictly software and with no hardware components to modify the spacecraft. The make up of the experiment leverages ISS assets and NASA - Ames Research Center's Astrobee mission control center. Overall the research done is educational in nature and adds value to NPS students through Masters thesis exposure to flight experimentation. Guest Scientist Research is a pivotal make up for the ISS and as such is the ideal platform to conduct propellantless hopping maneuvers. Requested services onboard the ISS are Astronaut Support for limited Astrobee handling (Astrobee is expected to be autonomous), video footage of the experiment, and data uplink/downlink capabilities.

D. FLIGHT REQUIREMENTS

No additional flight hardware. Experiments use Astrobee free-flyer onboard ISS. ASTROBATICS only requires to uplink a software executable to the Astrobee free-flyer. On-orbit experimentation required to demonstrate and validate hopping maneuver in the relevant dynamic environment. Hardware-related dynamic effects, such as contacts dynamics, are difficult to accurately recreate on a simulation environment. Experiments on a numerical simulation and on a reduced dynamic environment on the lab. have already been conducted.

E. TRANSITION PLAN

Use of NASA - Ames Research Center's Astrobee control center to command and downlink experiment data. PI receives experiment data and is responsible for analysis and dissemination. Scientific results published as peer-reviewed publications in top-ranked journals and scientific conferences. Astronautical Engineering Masters students' involvement during the development, operations, and analysis.

F. MILITARY RELEVANCE

Improved robotics capabilities for on-orbit servicing or assembly. Unique inter-spacecraft transport capability. More capable/reliable/resilient space assets for national security as a result. Objects in space are increasing yearly. With each new satellite brings additional space debris that clutters the orbital planes. Military assets could use the servicing robot as an extra set of eyes on orbit. The options are endless. A camera could give real-time telemetry to display all hazards near the satellite. The camera could range from a real-time picture to an inferred sensor. The robot would have the agility to reposition itself in any orientation around the satellite to provide better viewing of potential obstacles. The servicing satellite could exam the physical condition of the target satellite to give visual feedback of the current condition of the satellite. This would provide vital information to ground crews to assess any repairs. Servicing vehicles would have installed dexterous arms that could complete rudimentary repairs as needed to further the life of the mission.

THIS PAGE INTENTIONALLY LEFT BLANK

VI. CONCLUSIONS

The hopping mobility approach for a muiltibody spacecraft was investigated. A hopping maneuver to be conducted on-board the International Space Station was designed for the platform, Astrobee. Software simulations were designed an executed to explore the hopping. The research question of this thesis, "Is there an ideal mobility for use in space that uses zero propellant?" The results of this thesis indicate that hopping mobility for use in space is not only a feasible option but that it can provide a zero propellant option for mobility in space. The next section addresses further research needs to accomplish a successful hopping maneuver in space.

A. FUTURE WORK

Future work includes further ground based experiments. The purpose of ground based experiments is to verify the concept of a hopping maneuver. Two facilities are available for ground based testing, one at NPS and another at NASA - Ames Research Center. The two centers provide a granite monolith table for near frictionless surface representative of the zero gravity environment of space. The SRL's testbed facility (Figure 31) is composed of three systems, 1) VICON motion capture system, 2) a 4x4 meter granite monolith table with attached 3D printed ISS handrails, 3) multibody FSS.

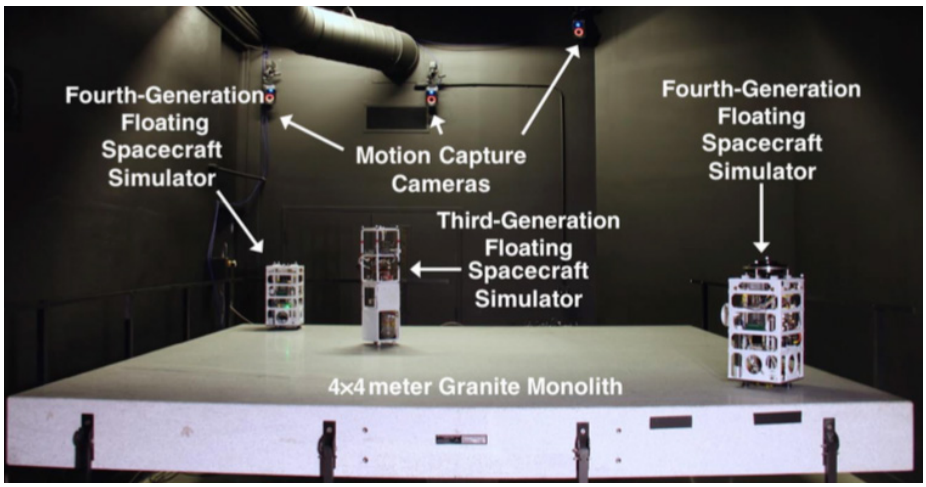

Figure 31. POSEIDYN Testbed. Source: Virgili-Llop (2016).

The 3D printed model of Astrobee's manipulator arm was created by fellow thesis student, Justin Komma to provide a real-world test platform to test hopping maneuver on NPS test-bed and compare with simulation results. The replica of Astrobee's robotic manipulator was mounted in such a way that the hopping mobility approach could be tested with hardware in the loop.

Due to the delays in the launch of Astrobee flight units to the ISS, the hopping mobility experiment in the ISS was not able to be conducted prior to the completion of this thesis. All paperwork and ground work has been completed in anticipation for the ISS experiment. Follow on work includes a more detailed concept of operations for the ISS experiment. Following the ISS experiment, further analysis will need to be conducted on the accuracy and propellant savings the hopping mobility maneuver saves if any.

B. RESEARCH SIGNIFICANCE

The mobility approach of this thesis has implementation for providing resilience and more capable space assets. Astobatics demonstrates the flexibility of on-orbit repurposing and augmentation of spacecraft. The ability to free-fly propellantlessly could enable the servicing of spacecraft in the form of refueling. Astrobatics would enable a space spacecraft to further the capabilities of national assets in the form of on-orbit assembly. Large apertures or large structures would no longer need to be assembly by an astronaut but rather a small dexterous multifaceted vehicle would suffice to safely assemble all structures in space. Lastly, astrobatics would provide the resilience of spacecraft already on-orbit in the form of repairs and anomaly resolution. Small vehicles could maneuver into position to inspect the exterior of damaged satellites to provide real-time anomaly resolution.

Image a satellite that had complications in launch and is unable to make it to its desired orbit. What if the satellite could be assisted to its desired orbit? This could happen one of two ways. The first idea is for the satellite to use the onboard propellant to send it off into its target orbit. The satellite reaches the orbit but then has no fuel onboard to complete any mission. Now, insert a servicing satellite with the maneuvering capabilities developed at NPS. The servicing spacecraft could capture the tumbling spacecraft and with

its dexterous arms could then refuel the orbiting satellite enabling and further mission life. The second option is the servicing satellite captures the satellite at sub-orbit and the servicing satellite uses onboard propellant to boost both vehicles to desired orbit.

The amount of money spent on building and launching military satellites must be protected and preserved. A servicing satellite could provide additional fuel, preform on-orbit repairs, maneuver or manipulate the orbiting satellite into new configurations.

THIS PAGE INTENTIONALLY LEFT BLANK

LIST OF REFERENCES

Ambrose, Robert O., Hal Aldridge, R. Scott Askew, Robert R. Burridge, William Bluethmann, Myron Diftler, Chris Lovchik, Darby Magruder, and Fredrik Rehnmark. 2000. "Robonaut: NASA's space humanoid," in *Intelligent Systems and their Applications, IEEE* 15, no. 4 (July 2000): 57–63. https://ieeexplore.ieee.org/stamp/stamp.jsp?tp=&arnumber=867913.

Bradstreet, Andrew. 2017. "Design, Integration, and Testing of an Autonomous Multi-body Spacecraft Simulator for Low Gravity Hopping and Grasping." Master's thesis, Naval Postgraduate School. https://calhoun.nps.edu/.

Burdick, Joel, and Paolo Fiorini. "Minimalist Jumping Robots for Celestial Exploration," in *The International Journal of Robotics Research* 22, no. 7–8 (July 2003): 653–674. doi: 10.1177/02783649030227013.

Chen, Yongquan, Chengjiang Wang, Wenfu Xu, Huihuan Qian and Yangsheng Xu. 2013. "Survey of Mobility Approaches for EVR Application in Space Station," in *IEEE International Conference on Information and Automation (ICIA)* (August 2013): 493–498. doi: 10.1109/ICInfA.2013.6720349.

Coleshill, Elliott, Layi Oshinowo, Richard Rembala, Bardia Bina, Daniel Rey, and Shelley Sindelar. 2009. "Dextre: Improving Maintenance Operations on the International Space Station," in *Acta Astronautica* 64, no. 9 (2009): 869–874. doi: 10.1016/j.actaastro.2008.11.011.

Dubowsky, Steven, and Evangelos Papadopoulos, 1993. "The Kinematics, Dynamics, and Control of Free-Flying and Free-Floating Space Robotic Systems," In *IEEE Transactions on Robotics and Automation*, vol. 9, no. 5 (October 1993): 531–543. doi: 10.1109/70.258046.

Hockman, Benjamin J. and Mario Pavone. 2017. "Stochastic Motion Planning for Hopping Rovers on Small Solar System Bodies," in *Intentional Symposium on Robotics Research (ISRR)*, Puerto Varas, Chili, 2017. Puerto Varas, Chili, 2017.

Japan Aerospace Exploration Agency. 2017. "JEM Internal Ball Camera (Int-Ball)." http://issstream.tksc.jaxa.jp/iss2/press/170726_intball_en.pdf.

Keller, John. 2016. "DARPA RSGS Program Eyes Space Robot to Maintain Geosynchronous Satellites. (Defense Advanced Research Projects Agency) (Robotic Servicing of Geosynchronous Satellites)," in *Military & Aerospace Electronics* 27, no. 6 (June 1, 2016): 4.

Knight, Russell, Caroline Chouinard, Grailing Jones, and Daniel Tran. 2014."Leveraging Multiple Artificial Intelligence Techniques to Improve the Responsiveness in Operations Planning: ASPEN for Orbital Express." *AI Magazine* 35 (4): 26–36. http://dx.doi.org.libproxy.nps.edu/10.1609/aimag.v35i4.2555.

Komma, Justin. 2018. "Mechatronics: the development, analysis, and ground based demonstrations of robotic spacecraft hopping with a manipulator." Unpublished Thesis, December 14, 2018.

McCamish, Shawn B., Marcello Romano, Simon Nolet, Christine M. Edwards, and David W. Miller. 2009. "Flight Testing of Multiple-Spacecraft Control on SPHERES During Close-Proximity Operations." In *Journal of Spacecraft and Rockets*, vol 46, no.6 (December 2009): 1202–1213.

Morris, Jefferson. 2007. "Full Service: Pioneering Orbital Express Mission Offers Many Lessons for Future Satellite Servicing." *Aviation Week & Space Technology* 167, no. 4 (July 23, 2007): 57. http://search.proquest.com/docview/206168870/.

National Aeronautics and Space Administration. 2018. "Astrobee." Last modified October 10, 2018. https://www.nasa.gov/astrobee.

National Aeronautics and Space Administration. 2018. "International Space Station Basics." https://www.nasa.gov/pdf/179225main_ISS_Poster_Back.pdf.

National Aeronautics and Space Administration. 2018. "R2." Last modified October 22, 2018. https://robonaut.jsc.nasa.gov/R2/.

National Aeronautics and Space Administration. 2018. "Robonaut 2." https://www.nasa.gov/sites/default/files/fs201402002_jsc_robonaut2_fs_updates4.pdf.

National Aeronautics and Space Administration. 2018. "Pilot Study with the Crew Interactive Mobile Companion (Cimon) (Mobile Companion). Last modified July 19, 2018. https://www.nasa.gov/mission_pages/station/research/experiments/2684.html.

National Aeronautics and Space Administration. 2017. "Synchronized Position Hold, Engage, Reorient, Experimental Satellites (SPHERES)." Last modified July 26, 2017. https://www.nasa.gov/mission_pages/station/research/experiments/311.html.

Park, In-Won, Trey Smith, Hugo Sanchez, Sze Wun Wong, Pedro Piacenza, and Matei Ciocarlie. 2017. "Developing a 3-DOF Compliant Perching Arm for a Free-Flying Robot on the International Space Station," in *IEEE* International Conference on *Advanced Intelligent Mechatronics* (July 2017): 1135–1141.

Patten, Laryssa, Lindsay Evans, Layi Oshinowo, Marius Ochisor, Nara Kazuharu, Aris Lodewijk, and Ed Tabarah. 2002. "International Space Station Robotics: A Comparative Study of ERA, JEMRMS and MSS," in 7th ESA Workshop on *Advanced Space Technologies for Robotics and Automation* 'ASTRA 2002' (Noordwijk: ESA), 1–8. http://robotics.estec.esa.int/ASTRA/Astra2002/Papers/astra2002_1.3-1.pdf.

Rehnmark, Fredrik, Ivan Spain, William Bluethmann, S. Michael Goza, Robert O. Ambrose, and Ken Alder. 2004. "An Experimental Investigation of Robotic Spacewalking." *4th IEEE/RAS International Conference on Humanoid Robots, 2004*, 1:366–384. USA: IEEE, 2004. doi: 10.1109/ICHR.2004.1442132.

Sallaberger, Christian. 1997. "Canadian Space Robotic Activities." *Acta Astronautica* vol. 41, no. 4 (1997): 239–246. doi: 10.1016/S0094-5765(98)00082-4.

Shoemaker, James, and Melissa Wright. (2003). "Orbital Express Space Operations Architecture Program," in Proceedings of SPIE 5088, Space Systems Technology and Operations (Orlando, FL), 56–65. doi: https://doi.org/10.1117/12.499871.

Siciliano, B., Sciavicco, L., Villani, L., and Oriolo, G. (2010). *Robotics*. London :Springer-Verlag.

Smith, T., Barlow, J, Bualat, M., Fong, T., Provencher, C., Sanchez, H., and Smith, E. 2016. "Astrobee: A New Platform for Free-Flying Robotics on the International Space Station." *International Symposium on Artificial Intelligence, Robotics, and Automation in Space* (i-SAIRAS), 2016. http://hdl.handle.net/2060/20160007769.

Ticker, Ronald, Frank Cepollina, and Benjamin Reed. 2015. "NASA's In-Space Robotic Servicing." *AIAA Space 2015 Conference and Exposition*. 31 Aug. – 2 Sep. 2015, Pasadena, California. AIAA, 2015.

Ulamec, S., Kucherenko, V., Biele, J., Bogatchev, A., Makurin, A., and Matrossov, S. 2011. "Hopper Concepts for Small Body Landers." *Advances in Space Research* 47, no. 3 (2011): 428–439.

Virgili-Llop, Josep, Jerry V. Drew II, and Marcello Romano. 2016. "Design and Parameter Identification by Laboratory Experiments of a Prototype Modular Robotic Arm for Orbiting Spacecraft Applications," in 6th *International Conference on Astrodynamics Tools and Techniques (ICATT)*, 14–17 March 2016, Darmstadt, Germany, 2016.

Virgili-Llop, Josep, Katrina P. Alsup. 2018. SPART: SPAcecraft Robotics Toolkit. https://github.com/NPS-SRL/SPART. Available: https://github.com/NPS-SRL/SPART.

Wilde, Markus, Stephen Kwok Choon, Alessio Grompone, and Marcello Romano. 2018. "Equations of Motion of Free-Floating Spacecraft-Manipulator Systems: An Engineer's Tutorial." *Frontiers in Robotics and AI* 5:41. doi: 10.3389/frobt.2018.00041

Yoshida, Kazuya. 2003. "Engineering Test Satellite VII Flight Experiments for Space Robot Dynamics and Control: Theories on Laboratory Test Beds Ten Years Ago, Now in Orbit." *International Journal of Robotics Research* 22, no. 5 (May 1, 2003): 321–335. http://search.proquest.com/docview/230036725/.

INITIAL DISTRIBUTION LIST

1. Defense Technical Information Center
   Ft. Belvoir, Virginia

2. Dudley Knox Library
   Naval Postgraduate School
   Monterey, California